ORIGINAL PAPER

Open Access

Check for updates

Banded amphibolites in the Alps: a new interpretation in relation to early Paleozoic peraluminous magmatism

Roger Zurbriggen[1,2*]

Abstract

The Strona-Ceneri Zone is located south of the Insubric line, where Alpine overprint is mainly brittle and of low grade or even absent. Apart from the unmetamorphic Permo-Carboniferous sediments and intrusiva the Strona-Ceneri Zone is an Ordovician gneiss complex composed of paragneisses, migmatites, peraluminous orthogneisses and banded amphibolites associated with meta-gabbros and meta-ultramafics. Despite of the individual characters of the other Ordovician gneiss terranes north of the Insubric line, most prominently the Aar Massif, the Gotthard, Silvretta and Ötztal nappes, they show analogous lithological formations and pre-Mesozoic structures indicating similar genetic processes. A revision of geological maps and new field observations in these gneiss terranes indicate characteristic spatial relationships of banded amphibolite formations with migmatites and orthogneisses. The contrasting chemistries of the peraluminous rocks (para- and orthogneisses) and the basaltic amphibolites with a lack of intermediate lithologies in between can be explained by the setting of peraluminous arc magmatism within a subduction–accretion complex. In this model the amphibolites represent primary basalts which ponded at the base of the subduction–accretion complex and delivered the heat for the production of peraluminous melts. Volume estimations indicate a "zone of intermingling" composed of immiscible basalts and peraluminous melts with a total thickness of several kilometers. In this "zone of intermingling" the protoliths of the banded amphibolite formations were generated. Steep strike-slip faults, which are important structures for the syn-magmatic cratonization of subduction–accretion complexes, provide pathways for the emplacement of magmas, migmatites and intermingled materials. This results in the formation of steeply oriented sheets of orthogneisses, deformed migmatites and banded amphibolite formations, respectively. Finally, the paper lists many other peri-Gondwanan regions with an early Paleozoic peraluminous arc magmatism, indicating a similar setting on a global scale.

Keywords: Banded amphibolites, Pre-Mesozoic basements in the Alps, Cambro-Ordovician orthogneisses, Peraluminous arc magmatism, Cratonization of subduction–accretion complexes, Early Paleozoic Cenerian orogeny, I-S line

1 Introduction

Albert Heim (1921, p. 65) stated that "The Alps, despite of the many magmatic rocks, are not a magmatic orogen." Thus, the majority of magmatites is much older than the Alpine orogeny. They were generated either

(i) in late Paleozoic related to the formation of Pangaea and subsequent Permian transtension, or (ii) during the Ordovician orogeny at the periphery of Gondwana (Bussien et al. 2011; Zurbriggen 2015 and references therein). Von Raumer et al. (2015) and Villaseca et al. (2016), just to mention two of many more studies, developed comprehensive reconstructions of the early Paleozoic magmatic event, for which Zurbriggen (2017) has suggested the new term "Cenerian orogeny". The

Cenerian orogeny is distinctively different to the Pana-frican, Cadomian, Caledonian and Variscan orogenies, regarding timing, tectonic setting and paleo-latitude.

The geology of the Variscan and Cenerian orogenies is recorded in the pre-Mesozoic basement units of the Alps. Heim (1921, 1922) already described in detail their lithological and structural analogies, namely between the Helvetic Aar, Gotthard, Mont-Blanc, and Aiguilles Rouges massifs (pp. 234, 257), and between the Eastern Alpine crystalline basements of the Ötztal and Silvretta nappes and the Southern Alpine "Seengebirge", the Strona-Ceneri Zone (pp. 780, 820). A common structural feature of these units is the moderately to steeply dipping schistosity of the schists and gneisses. These are discordantly overlain by Permo-Carboniferous sediments, as described and drawn in the many profiles of Heim (1921, pp. 6, 46, 159, 160) and Heim (1922, pp. 823, 829, 830a).

The pre-Carboniferous schists and gneisses are also referred as "Altkristallin", a Swiss term which is still in use (Gnägi and Labhart 2015, pp. 89, 91) to denote the country rocks of the Variscan granitoids. In all of the above mentioned pre-Mesozoic basement units, the "Altkristallin" consists of paragneisses, migmatites, peraluminous orthogneisses, and banded amphibolites.

Regarding the Strona-Ceneri Zone, age data of Franz and Romer (2007 and references therein) indicate that accretion of the pelites and greywackes, eclogitization of the amphibolites, migmatization of the sediments, intrusion and deformation of the orthogneisses occurred in a remarkable short time interval of 12 Ma (462–450 Ma) and clearly indicate an Ordovician orogenic evolution for the Strona-Ceneri Zone. A similar geology is reported for other pre-Mesozoic basement units in the Alps: Schaltegger et al. (2003) indicate a time span of 35 Ma (480–445 Ma) including gabbroic intrusions (478 ± 5 Ma), their HP overprint followed by anatexis between 456 and 450 Ma in the Aar Massif. Ordovician ages of 460–470 Ma for eclogitic metamorphism subsequently followed by anatexis and magmatism are also reported for the Gotthard Nappe (Oberli et al. 1994; Mercolli et al. 1994) and for the Ötztal–Stubai Complex (Hoinkes and Thöni 1993; Thöny et al. 2008). The Silvretta Nappe shows similar rock associations (Schaltegger et al. 2003). Von Raumer et al. (2003) mention that in the Aiguilles Rouges/Mont-Blanc area magmatic ages of c. 450 Ma have been obtained for both, eclogitized basic rocks and orthogneisses.

There is consensus regarding the protoliths of the gneisses and migmatites. But the protoliths of the banded amphibolites are under discussion. Most studies interpret the banded amphibolites (i) as members of an ophiolite sequence due to their MORB signature (Buletti 1983) and association with eclogites and ultramafic rocks, or (ii) as bimodal metavolcanics due to their compositional banding (Giobbi Mancini et al. 2003). Both tectonic settings are supported by chemical analyses of case studies. But from a general perspective of subduction–accretion tectonics of the Ordovician orogeny (Zurbriggen 2017) they cannot serve as main setting due to following reasons: A clear ubiquitous ophiolite stratigraphy is lacking and obduction is the exception rather than the rule in accretionary complexes. Furthermore, a rhythmic alteration of acidic and basic layers of volcanic rocks might occur as local phenomenon but is unlikely to explain banded amphibolite formations over geographically large distances. By the way, the banded amphibolite formations are associated with gabbros indicating a plutonic rather than a volcanic environment, and Ordovician volcanism is dominated by rhyolites and dacites, but poor in andesites (Heinisch 1981).

This study provides new field observations from the Strona-Ceneri Zone and other pre-Mesozoic basements units from the Alps. It highlights the role of the banded amphibolite formations in the context of the widespread Ordovician anatexis and peraluminous magmatism. Furthermore, a comparison of studies from other peri-Gondwanan terranes indicates that peraluminous magmatism was a global phenomenon in early Paleozoic times. It was related to two factors: (i) An extraordinary large sediment input from the eroding Transgondwanan Supermountain (Squire et al. 2006) into (ii) a circum-Gondwanan subduction system (Rino et al. 2008). This triggered on a global scale the formation of subduction–accretion complexes, which cratonized during peraluminous magmatism (Zurbriggen 2017).

2 Methodology

2.1 The importance of rock volumes and the method to estimate percentages

Other than collisional orogens with subhorizontal nappes or continental arcs composed of complex spheroidal batholiths, cratonized subduction–accretion complexes create a steeply structured crust consisting of intercalated sheets of paragneisses, orthogneisses, migmatites and banded amphibolite formations (Zurbriggen 2015). This steep geometry and the fact that the lithologies generally show the same dip (thus, no correction necessary for different apparent thicknesses as a function of different dip angles), allows to estimate the volumetric rock percentages by estimating the map area percentages. This in turn, allows to make a couple of rough but fundamental calculations such as (i) the percentage of crustal versus mantle material, (ii) the amounts of peraluminous and metaluminous orthogneisses, and (iii) the amount of

hidden basalts necessary for the generation of migmatites and peraluminous granitoids.

Area percentages were gained by the following working procedure:

1. Maps of the areas of interest are copied.
2. The different lithologies are classified according to the predefined lithological groups. For this study four lithological groups were defined: orthogneisses, migmatites, paragneisses and amphibolites (including ultramafics).
3. The defined lithologies are cut out from the map copies with a scissor and the pieces are grouped accordingly.
4. All pieces of the same lithological group are weighted together with a high precision laboratory balance having an accuracy of 0.1 mg.
5. The total weight of all pieces of a lithological group is divided by the weight of a standardized piece with a known area, e.g. 100 km^2. By this normalization the amount of km^2 per lithological group can be calculated.
6. The absolute km^2 can be further calculated to a corresponding area %.

The accuracy of this weighting method is good. But the challenge is the quality of the maps and how lithologies are grouped and cut out. Therefore, (i) a careful working is needed and (ii) the numbers should be interpreted at a level of about ± 3 area%. However, this precision is good enough for rough volume estimations needed to describe an orogen and its major processes in a semi-quantitative manner.

2.2 The critical use of geochemical diagrams—descriptive versus tectonic discrimination

Von Raumer et al. (2003) classified the early Paleozoic orthogneisses inside and outside of the Alps according to Maniar and Piccoli (1989) as oceanic plagiogranites, rift-related granitoids, island arc granites, continental arc granites, continental collision granitoids and post-orogenic granitoids. They then concluded that the Cambro-Ordovician evolution was a sequence of oceanic and continental rifting followed by arc settings and a final collision, as indicated by some Ceneri gneisses plotting into the field of collisional granitoids (see caption of Figure 3b in Von Raumer et al. 2003). Other workers confirmed these tectonic settings by similar chemical discrimination plots with the result that in the literature the early Paleozoic orthogneisses are well established as rift-related and/or collisional related granitoids.

Here the fundamental criticism of Barker et al. (1992) must be considered. It is based on a case study in the Gulf of Alaska, where forearc granitoids were generated by the melting of flyschoid sediments (greywackes). These granitoids reflect compositions and isotopic signatures of their sedimentary source rocks, which themselves have inherited compositions and signatures of the eroded rocks in the hinterland. Barker et al. (1992) write at the end of their abstract: "These Alaskan granodiorites do not fit into the alphabetical classification of Australian workers. Being melts of sedimentary rocks, they should have S-type character. Because the source flysch is quartzofeldspathic and of arc origin, however, the granodiorite shows I-type character. Our results also highlight a problem with Pearce et al.'s (1984) and Harris et al.'s (1986) purportedly tectonic-discriminant plots for granitic rocks. These diagrams classify our granodiorites as "volcanic arc granite" and reflect their source rocks rather than their tectonic environment of origin."

Conclusively, it can be a misleading practice to apply genetically pre-interpreted tectonic discrimination diagrams to peraluminous granitoids generated by the melting of greywackes. In fact, Zurbriggen et al. (1997) has shown that the peraluminous orthogneisses of the Strona-Ceneri Zone show a Rb-(Y + Nb) pattern (Pearce et al. 1984), which is identical to the inherited volcanic arc signatures of their metasedimentary host rocks.

Winter (2010, p. 385) gives another important statement about an uncritical use of chemical discrimination diagrams to identify a standard tectonic setting: "I am not a great lover of classifications. In spite of having given you several (see his compilation in Table 18-4), I think classification force the lovely variability and continuity of nature into inappropriately neat compartments, and they commonly have the same effect on our thought processes."

In fact, the attraction of a straight forward geochemical granite classification let us forget that (i) the early Paleozoic granitoids are surrounded by metagreywackes with similar chemical composition and isotopic signatures, (ii) the majority of granitoid material derived by melting of these greywackes at deeper crustal levels, and (iii) greywackes themselves indicate an active margin scenario and not a rifting or collisional setting (Barker et al. 1992; Zurbriggen 2017).

This critical review of applying tectonic discrimination diagrams to peraluminous granitoids has led myself to favor the A-B plot of Debon and Le Fort (1988) for the purpose of discussing magmatic processes rather than pre-defined standard tectonic settings. The A-B plot is recommended for several reasons: (1) It is purely descriptive without tectonic interpretations. (2) It differentiates between metaluminosity and peraluminosity (A-factor) and felsicity and maficity (B-factor), which represent two key aspects for the discrimination of granitoid suites.

(3) All types of mafic inclusions have B-values > 200, but metasedimentary and gabbroic inclusions are differing by positive and negative A-values, respectively. (4) It is insensitive for the typical back-reaction of K-feldspar to muscovite in S-type granitoids (White and Chappell 1990), which creates a shift in the QAP diagram towards the tonalite field. (5) It allows to identify trends of magmatic processes such as hornblende fractionation (metaluminous series), migmatization, magma mixing and miscibility gaps. (6) Debon and Le Fort (1988) defined three descriptive classes of granitoids, ALUM (aluminous), ALCAF (alumino-cafemic) and CAFEM (cafemic) series, which are in some analogy to the genetical classification of Chappell and White's (2001) S-type, low-temperature I-type and high-temperature I-type, respectively. (7) Villaseca et al. (1998) further specified the A-B diagram with respect to peraluminous granitoids. (8) Finally, A-B plots are increasingly used by magmatic petrologist like Castro et al. (2009), Villaros et al. (2018), or García-Arias et al. (2018).

3 Geology of the Strona-Ceneri Zone

From all pre-Mesozoic basement units (see Fig. 1a) the Strona-Ceneri Zone is of special interest, because it is south of the Insubric Line, where Alpine metamorphism did not exceed subgreenschist facies conditions (Frey et al. 1974). Thus, any high-grade structures are of pre-Mesozoic origin, which is helpful for field studies of the banded amphibolites. However, in a 2–3 km distance from the Ivrea-Verbano Zone, the Strona-Ceneri Zone was overprinted during Permian magmatism along the Cossato-Mergozzo-Brissago Line. Zurbriggen (1996, p. 119) defined between Cannobio and Brissago the Nuova Pace Line, north of which the Strona-Ceneri Zone is tectono-metamorphically overprinted by the Permian events related to the Ivrea-Verbano Zone. Important to note is that the Ivrea-Verbano Zone is younger than the Ordovician orogeny, but its complicated uplift history caused moderate to strong tilting of certain regions in the Strona-Ceneri Zone, which is important for the reconstruction of the original orientation of the Ordovician and Variscan high grade structures (Handy et al. 1999). Key evidence comes from east of Lago Maggiore, where Permian strata overlay steeply dipping gneisses with a high angular unconformity. Zurbriggen (1996) did a field survey and measured at nine different locations in the Malcantone and Valtravaglia areas these unconformities (see also Figs. 10c and d in Handy et al. 1999). The statistics confirm the profiles in Heim (1922; Figs. 242, 243 and Tafel XXXIV). On page 823 Albert Heim states «… im ganzen Gebiet des Luganersees zwischen dem steil stehenden Altkristallin und dem flach transgredierenden Perm …»

Regarding the pre-Permian orientation of the Strona-Ceneri gneisses, the highly discordant Permian stata on top represent the most important reference.

Another reason to focus first on the Strona-Ceneri Zone (Fig. 1b) are existing studies on the chemistry, petrology and age of the Ordovician metagranitoids (e.g., Zurbriggen et al. 1997), the banded amphibolites (e.g., Pinarelli et al. 2008) which were partly overprinted in the eclogite facies during the Ordovician (Franz and Romer 2007), the main Ordovician metamorphism (e.g., Handy et al. 1999) and the Carboniferous Schlingen folding (Zurbriggen et al. 1998). The geology of the Strona-Ceneri Zone is discussed in more detail in Zurbriggen (2015).

In the following a summary of data of the Ordovician metagranitoids (orthogneisses; Table 1) and new field observation of the banded amphibolites (Figs. 1c, d, 2) of the Strona-Ceneri Zone are shown.

Looking at the geological map of the Strona-Ceneri Zone (Fig. 1b) one can observe a spatial association of metagranitoids with the major horizon of banded amphibolite along the border between the northern gneiss unit and the southern schist unit. The banded amphibolites are associated with garnet-bearing amphibolites, meta-eclogites and ultramafics and were denamed as "Strona Ceneri Border Zone" by Giobbi Mancini et al. (2003). These linearly arranged formations occur on both sides of Lago Maggiore and form km-scaled folds with steep fold axes, so-called "Schlingen". Three Schlingen folds are indicated with their axial planes as red dotted lines in Fig. 1b. Schlingen folds deform the compositional banding of the amphibolites and the main schistosity of the gneisses under amphibolite facies conditions at 321.3 ± 2.3 Ma (Zurbriggen et al. 1997).

The map differentiates between different types of Ordovician metagranitoids, which are characterized in detail in Table 1.

About 20 area % of the map are composed by Ordovician metagranitoids, which were classified into three types by Zurbriggen et al. (1997). Type 1 are hornblende bearing metatonalites like they crop out at Molinetto (Fig. 1c). Their signatures indicate a mantle heritage. However, they represent a 10% minority compared to types 2 and 3, which have crustal signatures and can be regarded as S-type granitoids according to Chappell and White (1974). Type 3, Ceneri gneisses represent inclusion-rich diatexites, which are characteristic for such gneiss terranes (Zurbriggen 2015).

The banded amphibolite of Ponte Falmenta (see Fig. 1b for location) is about 40 m thick and at its eastern end (in Val Cavaglio) it is intensively folded by the San Bartolomeo Schlinge. North of the Falmenta bridge a $3 \text{ m} \times 0.6 \text{ m}$ big talc-rich lens is contained in the banded amphibolite. The central part of the lens consists mainly

Fig. 1 **a** Map of Alpine belt (after Von Raumer et al. 2013) with high-lighted pre-Mesozoic basement units for which Ordovician orthogneisses and large-scale Schlingen folds are reported. **b** Geological map of the Strona-Ceneri Zone (after Boriani et al. 1990). The types of orthogneisses are defined in Table 1. (Abbreviations: C: Cannobio, F: Ponte Falmenta, E: location of eclogite sample from Franz and Romer (2007), SBS: San Bartolomeo Schlinge, MGS: Monte Giove Schlinge, GS: Gambarogno Schlinge). **c** Road profile of Molinetto (Villa Elisabeth, c. 1.5 km south of Cannobio, Italy). Sample Z135 (Swiss coordinates: 2′698′055/1′100′650) is a meta-Spn-Hbl-Bt tonalite (Zurbriggen 1996); sample Z137 (Swiss coordinates: 2′697′980/1′100′380) is a banded amphibolite (Zurbriggen 1996). **d** Typical banded amphibolite (Swiss coordinates: 2′698′074/1′100′083)
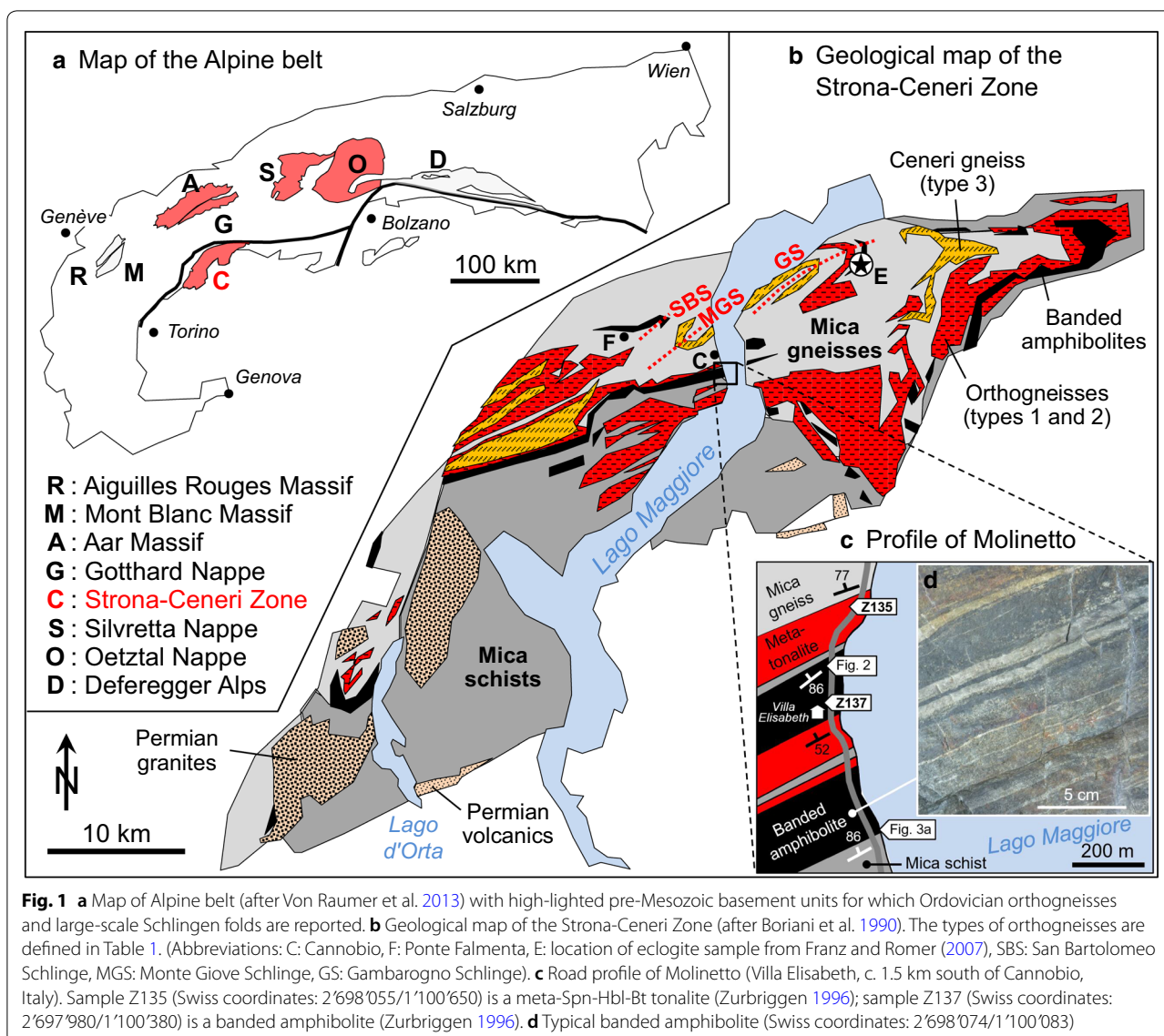
Table 1 Selected characteristics of the Ordovician metagranitoids of the Strona-Ceneri Zone (Southern Alps)

| Properties of Ordovician orthogneisses of the Strona-Ceneri Zone	Meta-quartz diorites, metatonalites	Metagranites, metagranodiorites	Augen gneiss	Ceneri gneiss	Meta-pegmatites
Mineralogical characteristics	Hbl bearing	Poor / free of Hbl	Kfs phenocrysts	Bt rich selvedges	Leucotonalitic, 0-15% Kfs
Zurbriggen et al. (1997)	Type 1 granitoids	Type 2 granitoids		Type 3 granitoids	
Outcrop area	3.0 %	9.5 %	2.1 %	6.3 %	< 0.1 %
Alkaline signature	Sodic	Mainly potassic			
$(^{87}Sr/^{86}Sr)_i$ Boriani et al. (1995)	<0.706; >0.708	>0.708	>0.708	-	-
Percentage of all metagranitoids	15 %	45 %	10 %	30 %	< 1%
	10 %	90 %			
I-S typology Chappell and White (1974)	I-type	S-type			
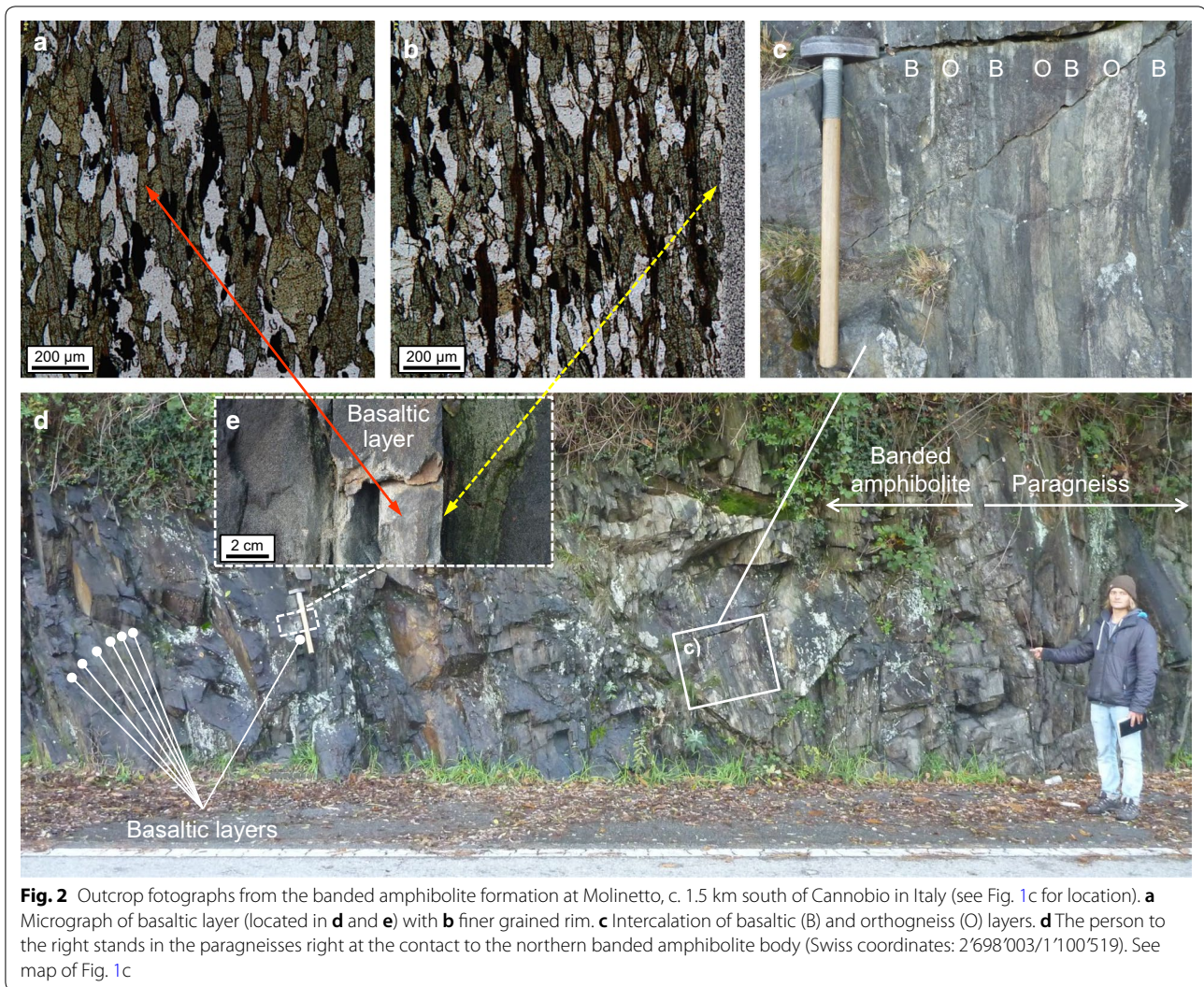
Fig. 2 Outcrop fotographs from the banded amphibolite formation at Molinetto, c. 1.5 km south of Cannobio in Italy (see Fig. 1c for location). **a** Micrograph of basaltic layer (located in **d** and **e**) with **b** finer grained rim. **c** Intercalation of basaltic (B) and orthogneiss (O) layers. **d** The person to the right stands in the paragneisses right at the contact to the northern banded amphibolite body (Swiss coordinates: 2′698′003/1′100′519). See map of Fig. 1c

of talc with some chlorite and serpentine. The talc minerals define a crude schistosity. Relics of anthophyllite and cummingtonite pre-date the replacement by talc. Anthophyllite indicates temperatures around 650 °C and might be coeval with the Ordovician main metamorphism or the Variscan Schlingen folding. Much larger anthophyllite-bearing ultra-mafic lenses occur in Val d'Isone, east of Lago Maggiore (Spicher 1940).

The amphibolites of the Strona-Ceneri Zone are strongly banded in all scales—from mm to meter scale and on a map-scale they are intercalated with metagranitoids, as can be observed along the 600 m road cut at Molinetto (Fig. 1c). In fact, at Molinetto there are two banded amphibolite bodies, a northern and a southern one. At the northern border of the northern amphibolite body (see map of Fig. 1c) the banding reveals to be a set of basaltic layers, each 5–10 cm thick with finer-grained rims (Fig. 2a, b, d, e), or an intercalation of basaltic and metagranitoid layers (Fig. 2c, d). The pervasive schistosity of the metagranitoid layers (denoted with "O" in Fig. 2c) indicates a significant deformation of a formerly more isotropic intercalation of the two materials, which is an important observation. In the southern amphibolite body, at the lake shore (same outcrop of Fig. 3a), one can observe distinct basaltic and coarser grained gabbroic layers. Locally these basaltic and gabbroic layers are boudinaged.

4 Comparison of pre-Mesozoic basements in the Alps

Similar relationships between banded amphibolites and orthogneisses or augen gneisses can also be made in the other pre-Mesozoic basements (Fig. 3). Figure 3b, c show the association of banded amphibolites with augen gneisses in an undeformed state. In the Aar Massif the
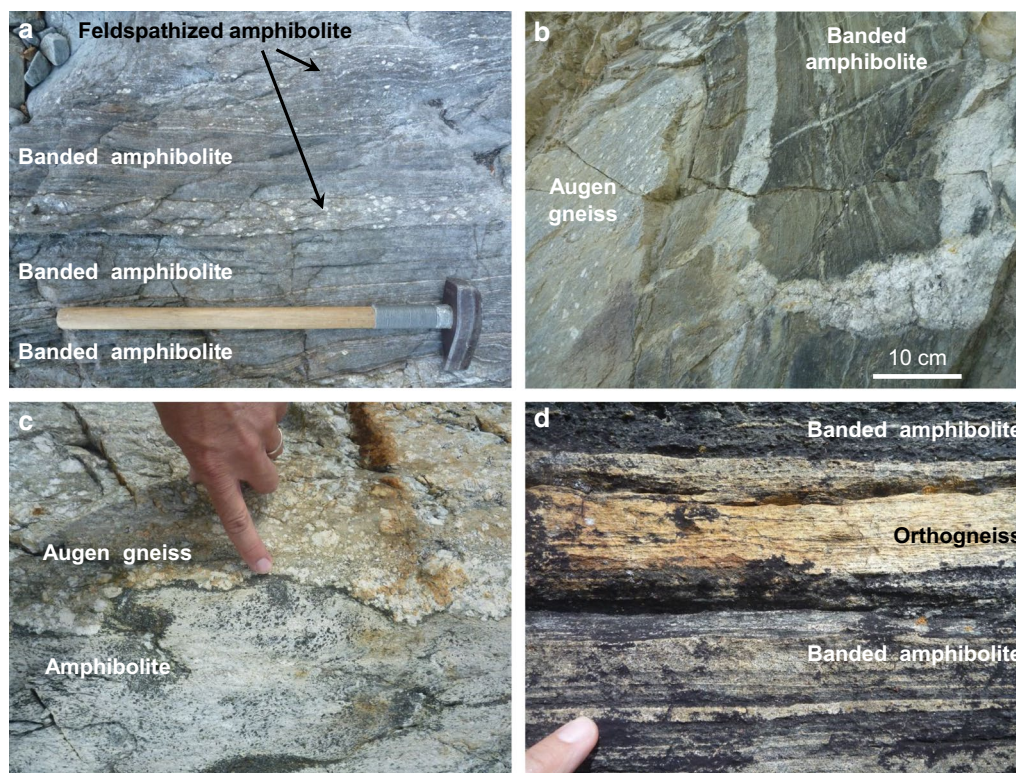
Fig. 3 Relationships between banded amphibolites and orthogneisses. **a** Feldspathized layers in a banded amphibolite (Strona-Ceneri Zone, south of Molinetto, Italy, Swiss coordinates: 2′698′120/1′100′035; for localization see also Fig. 1c). **b** Agmatite composed of schollen of banded amphibolite in a matrix of augen gneiss (Aar Massif, forest road from Betten Dorf to Martisberg, Valais, Switzerland, Swiss coordinates: 2′649′608/1′136′702). **c** Reaction rim between amphibolite and augen gneiss (Aar Massif, Chazulecher, Valais, Switzerland, Swiss coordinates: 2′647′461/1′139′792). **d** Banded amphibolite with intercalated layer of orthogneiss (Gotthard Nappe, Northwest of Lago die Dentro, Val Piora, Ticino, Switzerland, Swiss coordinates: 2′699′394/1′156′545)

banded amphibolites are obviously associated with migmatites as mapped by Labhart (1977) and Abrecht (1994) and shown in Fig. 4. Trails of schollen amphibolites (agmatites) grade into banded amphibolites indicating that the banding generates with increasing shearing. Amphibolitic agmatites in a matrix of augen gneiss (Fig. 3b) or intermingling structures between augen gneiss and amphibolitic schollen with reaction rims (Fig. 3c) indicate the simultaneous presence of basaltic and felsic materials. Figure 3d shows an intercalation of orthogneiss with banded amphibolite in the Gotthard Nappe, as observed in the Strona-Ceneri Zone, as well (Fig. 2c).

The banding of the amphibolites is an intrinsic character with a fractal pattern, manifested at all scales, from millimeter to kilometer. Figure 4 gives an impression how banded amphibolite formation can be intercalated on a map scale with migmatites. In the Silvretta Nappe (Zernez area), like in the Strona-Ceneri Zone (see Sect. 3) a similar intercalation on a map-scale can be observed between banded amphibolites and orthogneisses. Bächlin (1937), Spicher (1940), and Graeter (1951), who mapped the Swiss part of the Strona-Ceneri Zone east of Lago Maggiore referred to literature of the Silvretta Nappe, where similar amphibolites and relationships with para- and orthogneisses were described. But none of the pre-Mesozoic basement units contains more amphibolites (22% of the map area) than the Silvretta Nappe. These amphibolite formations alternate with long-shaped bodies of ortho- and paragneisses. This map-scale interlayering produces peculiar patterns in the entire area north of Zernez. Important observations in a 200 m thick banded amphibolite formation can be made along the road cut south of the Sassella road gallery (c. 4.5 km north of Zernez). What is mapped as one unit reveals to be a large variety of lithologies such as banded amphibolites, gabbros and interminglings of coarse gabbros with fine-grained basalts intruded by tonalites, Grt bearing amphibolites grading into paragneisses, aplites, and sets of several cm thin basaltic layers (metadykes) in a matrix of paragneisses (Fig. 5). This road profile
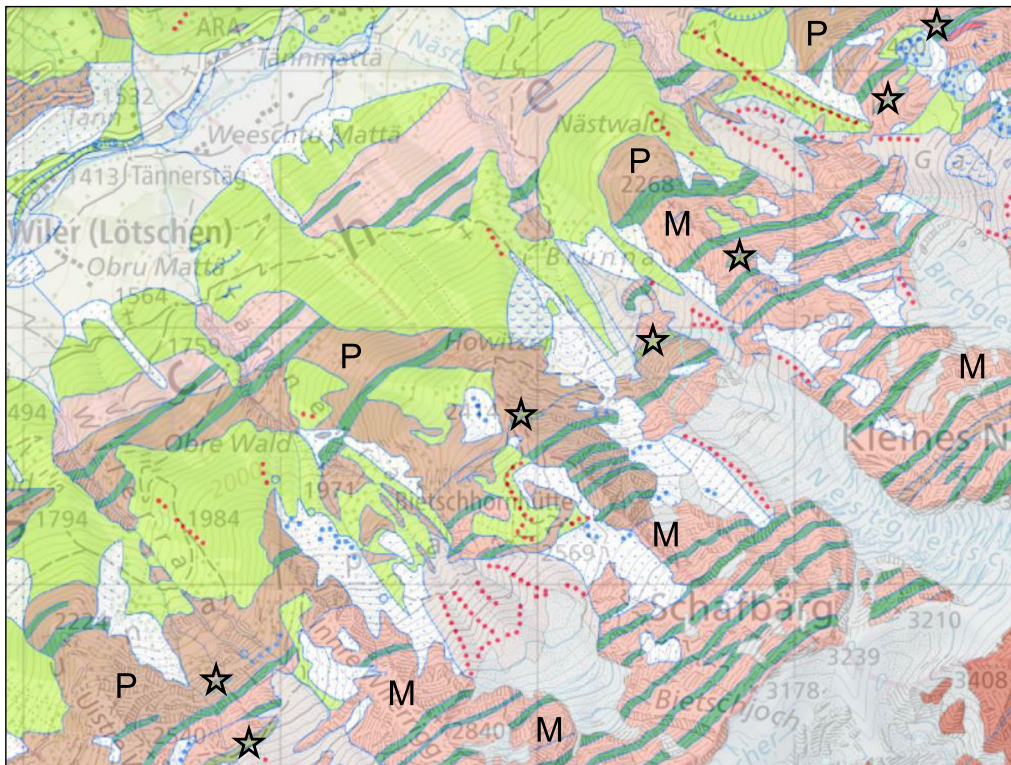
Fig. 4 Extract from the geological map of Lötschental, between Wiler (Swiss coordinates: 2′626 516/1′139 256, 1419 m) and Schafbärg (Swiss coordinates: 2′630 084/1′137 787, 3239 m). It shows the characteristic intercalation of banded amphibolite formations (green bands) and associated ultramafic bodies (indicated by stars) with migmatites (M) and paragneisses (P) (Source: GeoCover from https://map.geo.admin.ch)

displays the large lithological variety within banded amphibolite formations.

As argued in Chapter 2.1 the estimation of the volumetric proportions of the orthogneisses, migmatites, paragneisses and amphibolites is an important aspect in the investigation of the "Altkristallin". The statistical analysis (Table 2 and Fig. 6) reveals that c. 20% of these gneiss terranes are peraluminous orthogneisses and another c. 8% are migmatites. C. 7% are banded amphibolite formations, whereas their abundance can strongly vary from c. 2% in the Strona-Ceneri Zone to c. 22% in the Silvretta Nappe. The majority of banded amphibolite formations in all of these gneiss terranes is associated with meta-gabbroic and meta-ultramafic rocks. Therefore, they have a plutonic origin and are so-called "ortho-amphibolites".

5 Geochemistry and mineralogy of rocks from the Strona-Ceneri Zone

This study is reviewing published geochemical data. The references are given in the captions of Figs. 7, 8, 9.

The majority of the Ordovician orthogneisses of the Strona-Ceneri Zone are potassic granites, granodiorites and tonalites. Their minor elements (Rb vs. $Y + Nd$) indicate, according to Pearce et al. (1984) a volcanic arc signature, and the strontium isotope signatures (Boriani et al. 1995) classifies 90% of them, according to Chappell and White (1974) as S-types (Table 1).

In order to investigate the chemical relationships between orthogneisses, migmatites, paragneisses and amphibolites, samples of all these major lithologies where plotted in an A-B diagram of Debon and Le Fort (Debon and Le Fort 1988; Fig. 7). For reference, the mean compositions of a greywacke and a pelite (after Pettijohn 1963), a mean basalt (after Le Maitre 1976), I-type granitoids of the Lachlan Fold Belt (Chappell and White 1992) and the diorite-tonalite series of the Fusht Complex (Southern Oman; see Fig. 15 for location; data from Hauser and Zurbriggen 1994) are plotted, as well. Both, the Fusht Complex, a 790 Ma old Pan-African pluton (Mercolli et al. 2006) and the Lachlan I-type granitoids represent CAFEM suites (according to Debon and Le Fort 1988), which generated by fractionation of hornblende from more mafic precursors.

The paragneisses of the Strona-Ceneri Zone (metapelites and metagrewackes) define a compositional field (grey field in Fig. 7) with A-values from 10 to 200 and B-values from 50 to 210.
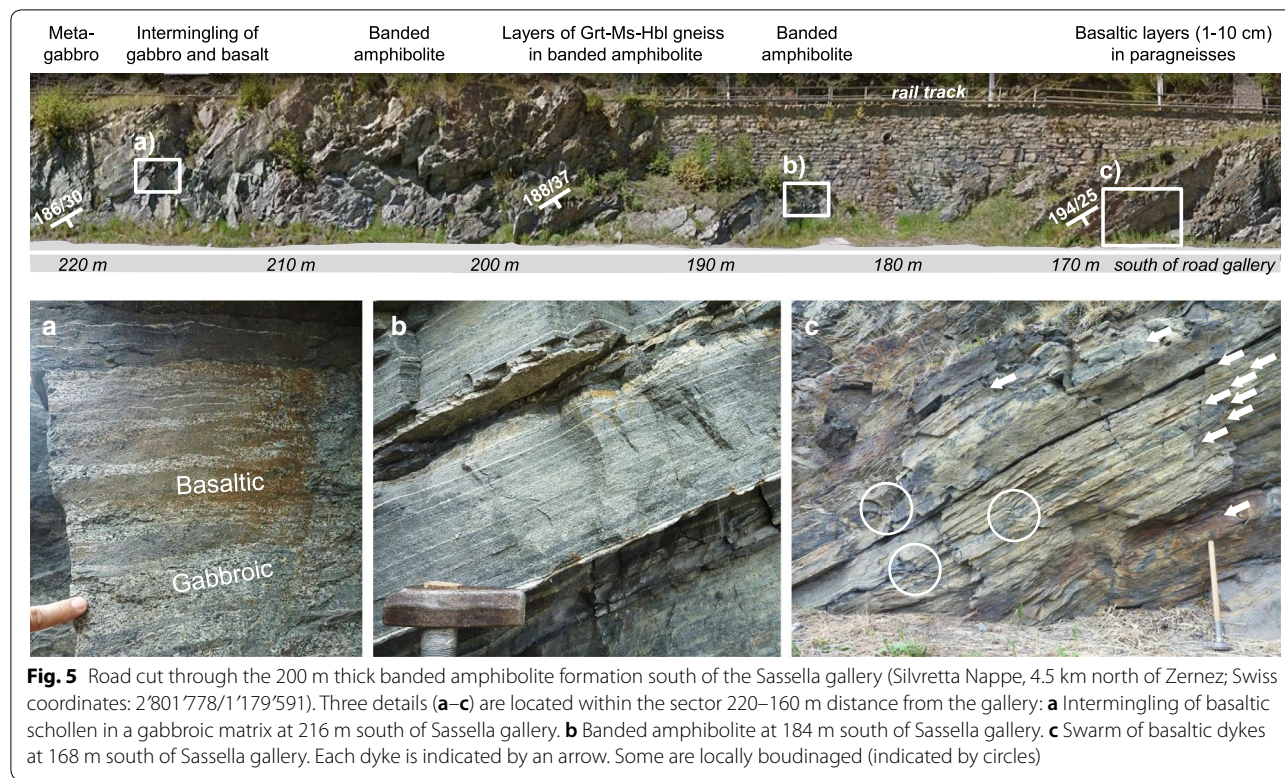
Fig. 5 Road cut through the 200 m thick banded amphibolite formation south of the Sassella gallery (Silvretta Nappe, 4.5 km north of Zernez; Swiss coordinates: 2′801′778/1′179′591). Three details (**a**–**c**) are located within the sector 220–160 m distance from the gallery: **a** Intermingling of basaltic schollen in a gabbroic matrix at 216 m south of Sassella gallery. **b** Banded amphibolite at 184 m south of Sassella gallery. **c** Swarm of basaltic dykes at 168 m south of Sassella gallery. Each dyke is indicated by an arrow. Some are locally boudinaged (indicated by circles)

Table 2 Square km and area percentages per main lithology from the different pre-Variscan gneiss units
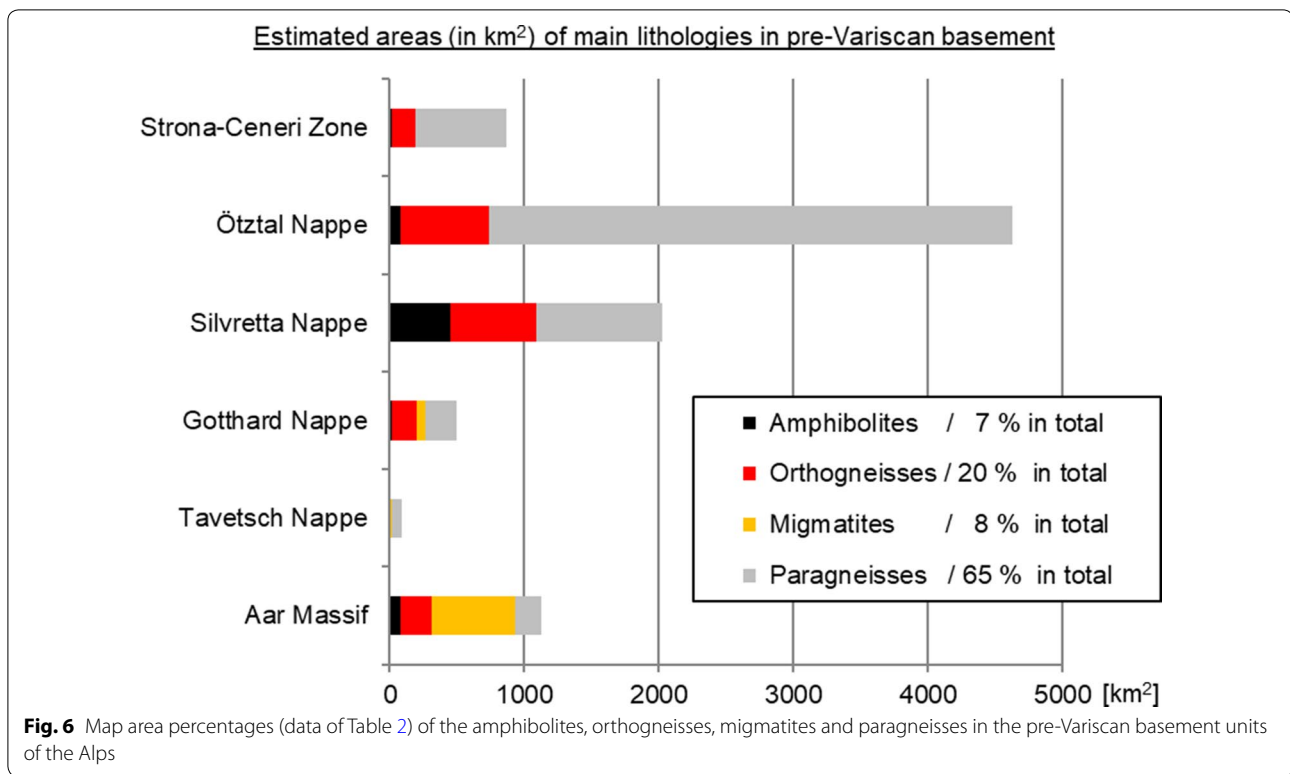
	Aar Massif	Tavetsch Nappe	Gotthard Nappe	Silvretta Nappe	Ötztal Nappe	Strona-Ceneri Zone	Sum
Amphibolites	82 km^2 7.3%	0.1 km^2 0.1%	16 km^2 3.2%	447 km^2 22.0%	81 km^2 1.7%	17 km^2 2.0%	643 km^2 7%
Orthogneisses	229 km^2 20.3%	0 km^2 0%	184 km^2 37.1%	645 km^2 31.8%	659 km^2 14.2%	173 km^2 20.0%	1890 km^2 20%
Migmatites	622 km^2 55.0%	18 km^2 20.2%	66 km^2 13.3%	0 km^2 0%	0 km^2 0%	0 km^2 0%	706 km^2 8%
Paragneisses	197 km^2 17.4%	71 km^2 79.7%	230 km^2 46.4%	939 km^2 46.2%	3892 km^2 84.0%	675 km^2 78.0%	6004 km^2 65%
Sum	1130 km^2 100%	89 km^2 100%	496 km^2 100%	2031 km^2 100%	4632 km^2 100%	865 km^2 100%	9243 km^2 100%

The data is plotted in the diagram of Fig. 6. Analysis is based on data taken from Zurbriggen (2015) for the Strona-Ceneri Zone, Geological Map of Switzerland, 1:500,000 (2008) for the Silvretta Nappe, Egger et al. (1999) for the Ötztal Nappe, and Berger et al. (2016) for the Aar Massif, Tavetsch Nappe and Gotthard Nappe. Note: In case of the Aar Massif, the Gärsthorn Gneiss Complex was classified as orthogneiss, Guttanen and Lötschental Gneiss Complexes as paragneisses, and the Ofenhorn-Stampfhorn, Erstfeld, Innertkirchen-Lauterbrunnen and Massa Gneiss Complexes as migmatites

The (strongly) peraluminous inclusion-rich Ceneri gneisses (type 3 orthogneisses, red X-symbols) plot into the left half of the grey paragneiss-field. Thus, Ceneri gneisses have identical composition than their host rocks, from which they derived by anatexis to form diapirs of diatexites. The Ceneri gneisses, and similar Ceneri gneiss-like lithologies of the other pre-Mesozoic basement units are ferrosilicic orthogneisses (Zurbriggen 1996). Ferrosilicic magmas are generated by near-total melting of metagreywackes at temperatures of at least 1000 °C (Castro et al. 2009).

The metatexites of the Strona-Ceneri Zone (formed at a lower degree of melting) form leucosomes and melanosomes, which differentiate by their B-values, along the brown dashed line with the two arrowheads. Mobilized leucosomes formed pegmatites (yellow crosses), which

Fig. 6 Map area percentages (data of Table 2) of the amphibolites, orthogneisses, migmatites and paragneisses in the pre-Variscan basement units of the Alps

plot at very low B-values in the field "felsic peraluminous". Both, metapegmatites and Ceneri gneisses are related to the anatexis of paragneisses and are therefore grouped together as type 3 orthogneisses.

Type 2 orthogneisses plot into the paragneiss-field and to the left of it into the field "felsic peraluminous", especially the augen gneisses. With some exceptions, type 2 and type 3 orthogneisses plot into the S-type field (above the green stippled I-S line).

Type 1 orthogneisses bear hornblende and plot as both, S- and I-types. The latter are metaluminous. But unlike the metaluminous Fusht Complex, there are no mafic members with B-values > 160 associated with the orthogneisses.

The fourth lithological formation, the amphibolites (Grt amphibolites and dark bands of banded amphibolites) plot far from the ortho- and paragneisses and migmatites. They have B-values between 250 and 410 and A-values mostly < − 100. In the AFM plot (Fig. 8) they reveal both, tholeiitic and calc-alkaline compositions. However, before attributing standard tectonic settings according to the AFM plot it is suggested to depict the field observations and the lithological variety within banded amphibolite formations, as will be discussed in Chapter 6.2.
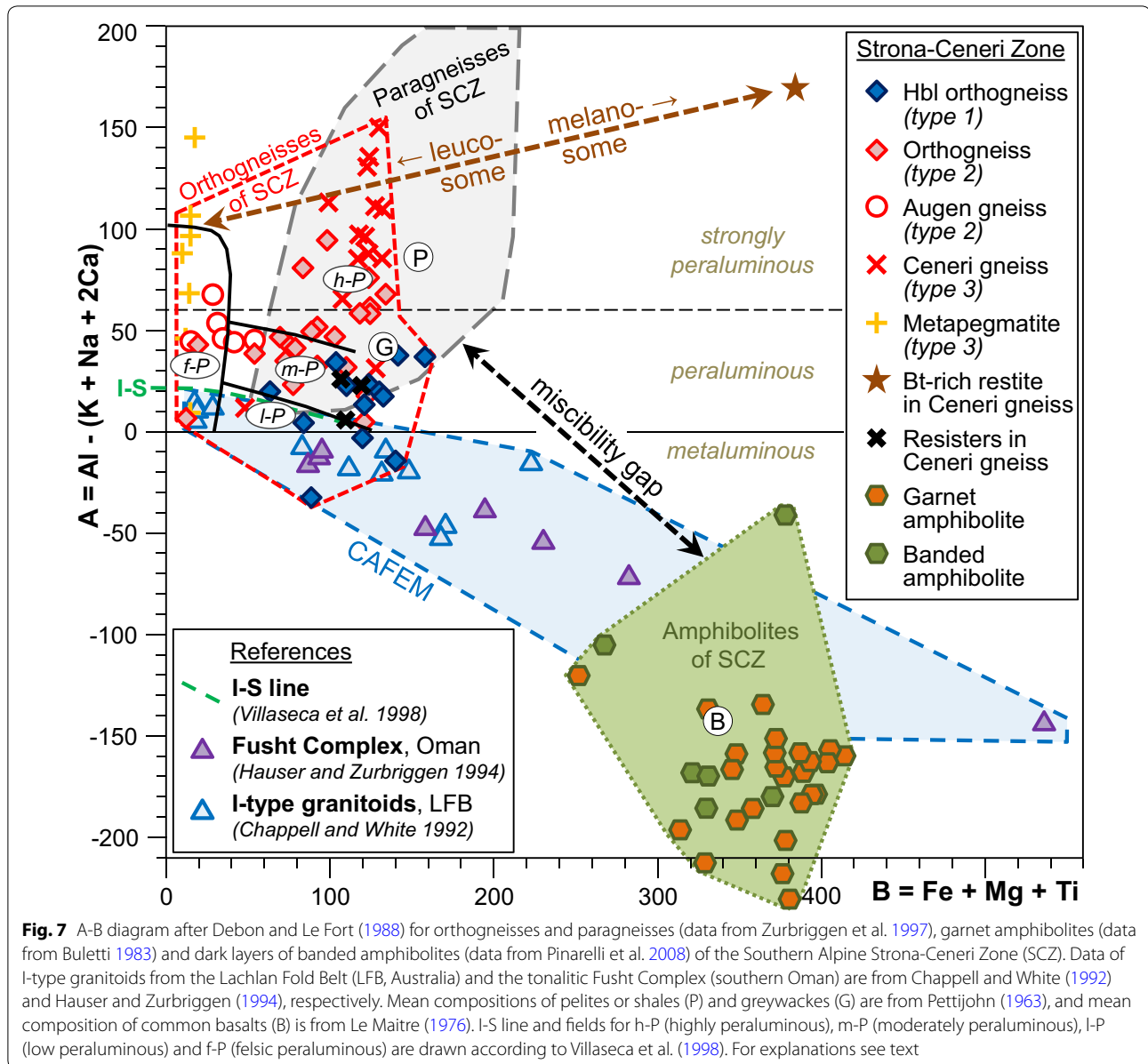
The orthogneisses of the Strona-Ceneri Zone are strongly related to the paragneisses, they lack mafic microgranular enclaves and are poor in mafic members. The same can be observed for the orthogneisses of the other pre-Mesozoic basement units in the Alps (Zurbriggen 2015). These characteristics are typical for peraluminous arcs in cratonizing subduction–accretion complexes as shown in Fig. 9, a compilation of batholith types from different settings. The diagram is taken from Villaseca et al. (1998) and modified as follows: The group of continental arcs is completed with the Fusht Complex. The Lachlan Fold Belt and the Strona-Ceneri Zone are according to Zurbriggen (2015) attributed to the setting of subduction–accretion complexes. Important to note are the percentages of the mafics, such as gabbros and diorites. They are very rare in peraluminous magmatic suites of subduction–accretion complexes.

6 Discussions

6.1 Discussion of the early Paleozoic peraluminous magmatism

It could be shown that c. 20 area % of the steeply structured Strona-Ceneri Zone consist of peraluminous orthogneisses, which are almost entirely (> 90%) composed of crustal material. Similarly, about 20 area% of the pre-Variscan gneiss terranes of the pre-Mesozoic basement units are peraluminous orthogneisses (Fig. 6), mostly S-types (Zurbriggen 2015). According to Fig. 6

Fig. 7 A-B diagram after Debon and Le Fort (1988) for orthogneisses and paragneisses (data from Zurbriggen et al. 1997), garnet amphibolites (data from Buletti 1983) and dark layers of banded amphibolites (data from Pinarelli et al. 2008) of the Southern Alpine Strona-Ceneri Zone (SCZ). Data of I-type granitoids from the Lachlan Fold Belt (LFB, Australia) and the tonalitic Fusht Complex (southern Oman) are from Chappell and White (1992) and Hauser and Zurbriggen (1994), respectively. Mean compositions of pelites or shales (P) and greywackes (G) are from Pettijohn (1963), and mean composition of common basalts (B) is from Le Maitre (1976). I-S line and fields for h-P (highly peraluminous), m-P (moderately peraluminous), l-P (low peraluminous) and f-P (felsic peraluminous) are drawn according to Villaseca et al. (1998). For explanations see text

the ratio of orthogneisses to paragneisses is 20:65. If the migmatites are counted with the orthogneisses, then the ratio of fully and partially molten rocks to paragneisses is 28:65. The paragneisses represent the crustal material in subduction–accretion complexes (Zurbriggen 2015), which by anatexis delivers the peraluminous magmas for the orthogneisses. Conclusively, about 25% of the paragneisses must melt to produce this volume of orthogneisses and migmatites. Assuming a thickness of the accretionary complex of 25 km, then the lowermost 6.25 km of the accreted greywackes and pelites must melt. In case the complex is 30 km thick, then a basal layer of 7.5 km must entirely melt.

Assuming upper amphibolite facies conditions at the base of a 30 km thick accretionary complex the anatectical layer must be additionally heated by 200 °C to reach at least 850 °C, the minimum temperature for the production of large volumes of granites (Aranovich et al. 2014).

The necessary heat must have been contributed by mantle-derived basalt of a similar volume as estimated by Barker et al. (1992) and Aranovich et al. (2014). The latter critically discuss the literature about granite producing processes and reach the following conclusions: Firstly, melting by dehydration of micas and amphiboles is not delivering the necessary volumes. Secondly, the
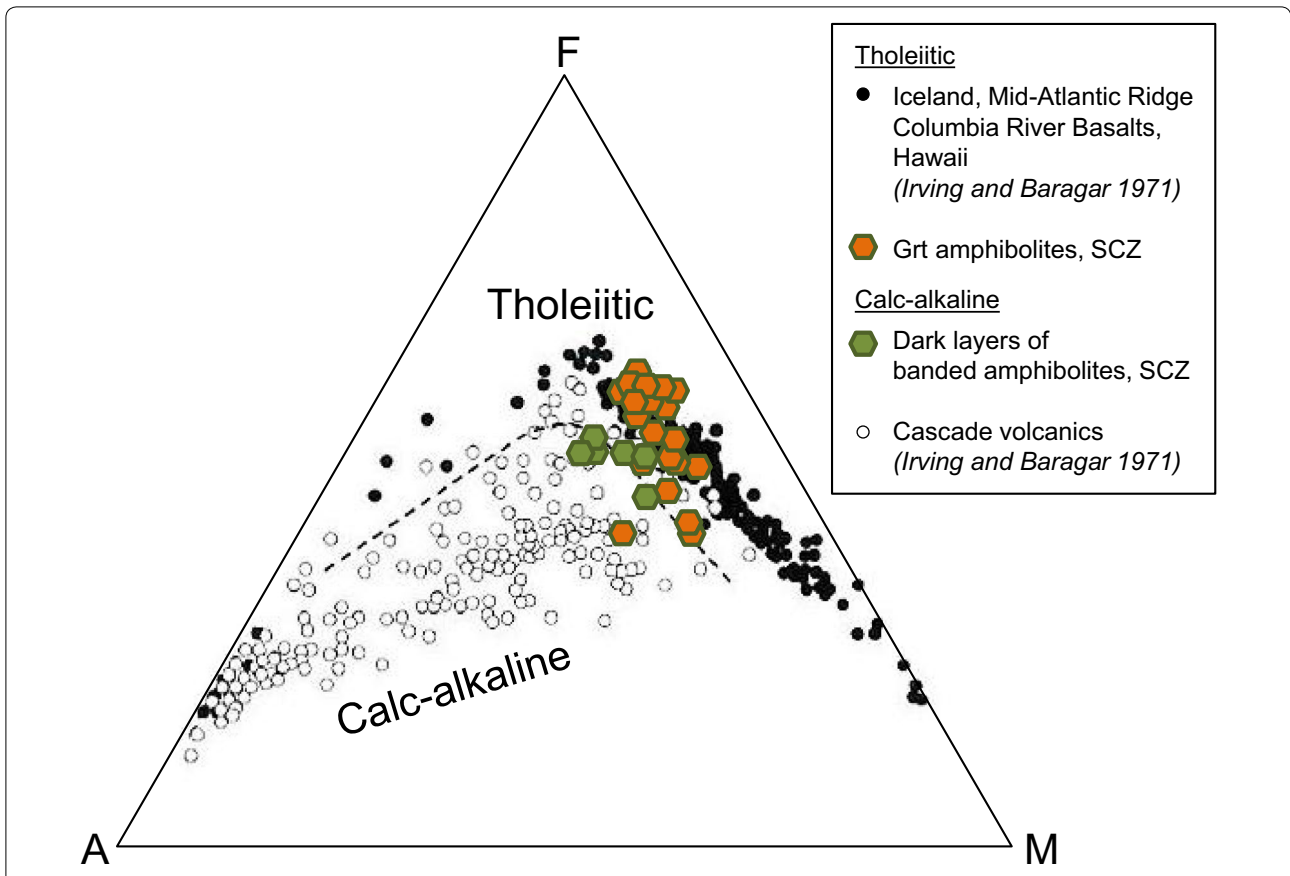
Fig. 8 AFM diagram (Irving and Baragar 1971) showing composition of banded amphibolites and garnet amphibolites of the Strona-Ceneri Zone (SCZ). Data for Grt amphibolites are from Buletti (1983). Data for dark layers of banded amphibolites are from Pinarelli et al. (2008)
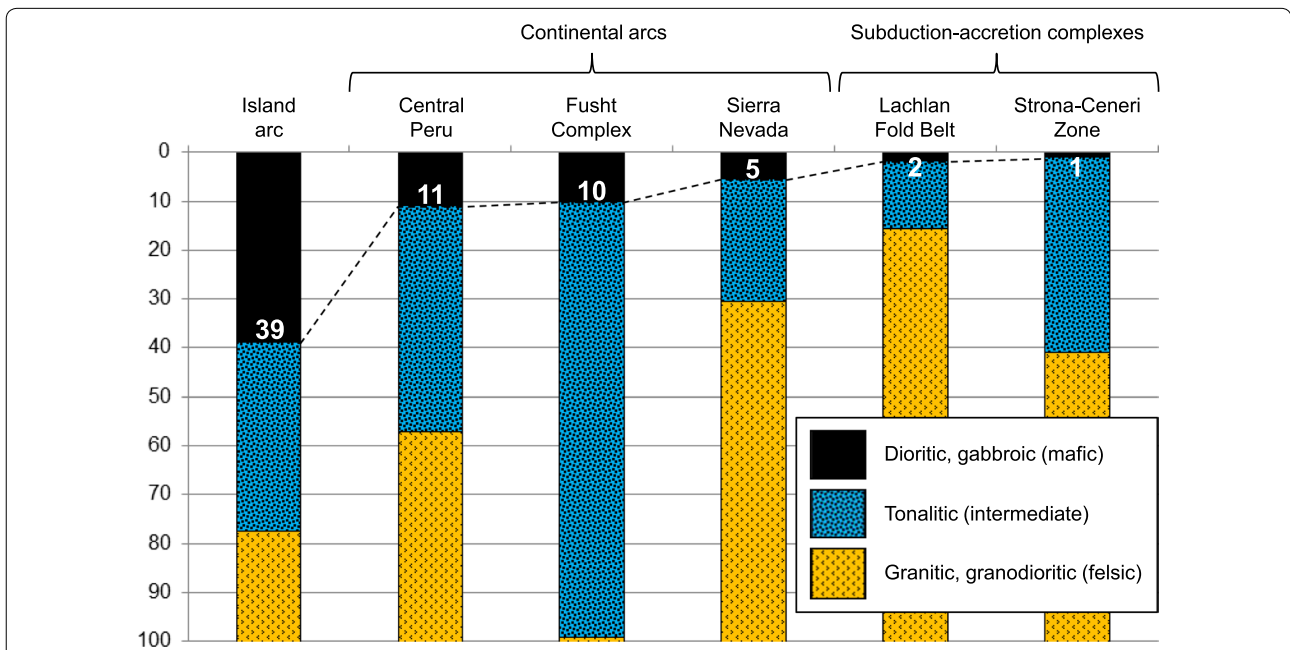

Fig. 9 Percentages of mafic (indicated by numbers), intermediate and felsic intrusiva in batholiths of three different settings: (i) island arc, (ii) continental arc and (iii) subduction–accretion complex. Data are from Villaseca et al. (1998), Hauser and Zurbriggen (1994) for the Fusht Complex, and Zurbriggen (2015) for the Strona-Ceneri Zone

Table 3 Sources of material and heat, and processes of peraluminous arc magmatism in subduction–accretion complexes

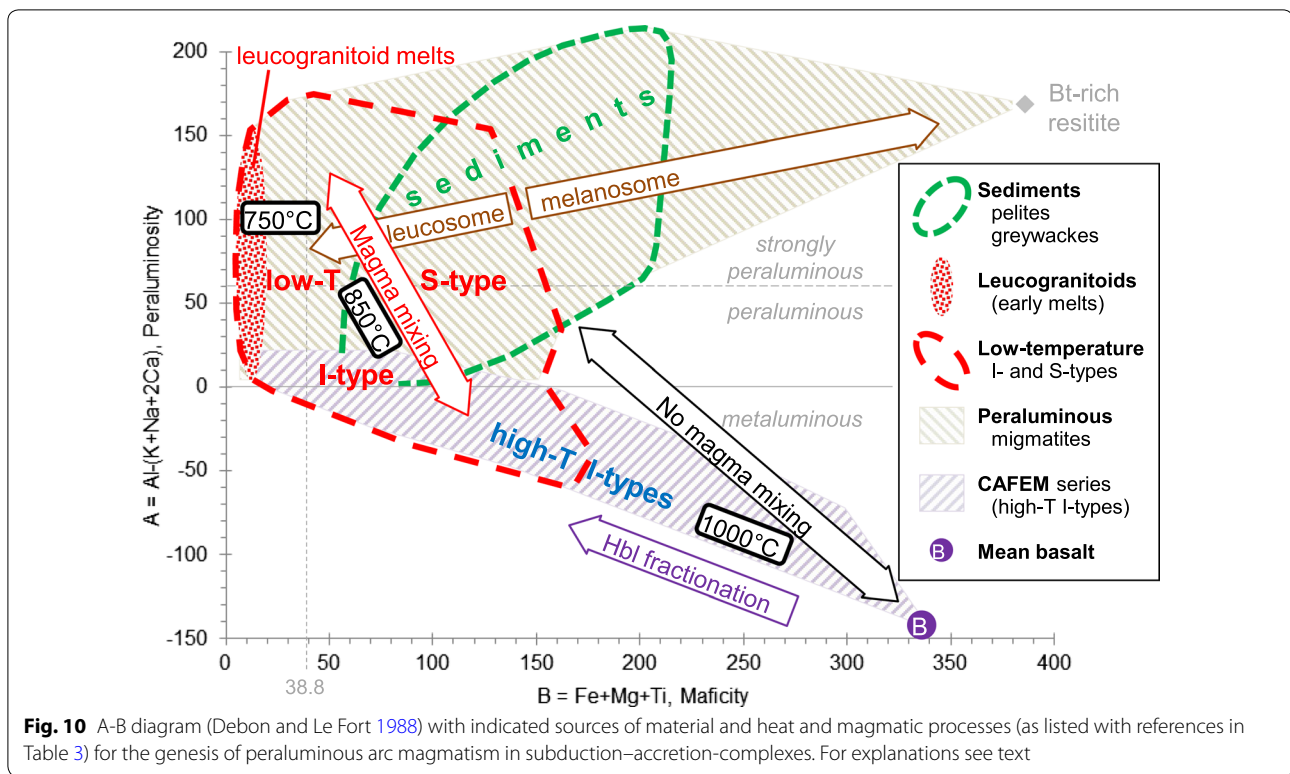|		
Material sources	Pelites, greywackes	Large amounts of (strongly) peraluminous S-type melts are generated in a temperature range between 850 and 875 °C (Vielzeuf and Holloway 1988)
	Basaltic rocks	Hbl bearing tonalites (high-temperature I-types, Chappell et al. 2004) and banded amphibolites indicate basaltic source rocks
Magmatic processes	Hornblende fractionation	Crystallization of hornblende is a major fractionation process in CAFEM series (Debon and Le Fort 1988)
	Dehydration melting	Muscovite dehydration melting can produce leucosomes of metatexites and pegmatites, thus, biotite dehydration is necessary to produce diatexites allowing for diapirism (Vielzeuf and Holloway 1988)
	Mixing of compatible magmas	Felsic magmas (B < 170) with similar viscosities at similar temperatures of c. 850 °C are compatible and can mix
	Heat transfer between incompatible magmas	Mantle-derived mafic magmas begin to solidify at 900 °C. Due to viscosity contrast they cannot mix with anatectical melts (Barker et al. 1992)
Heat source	Mantle	Hot mantle and/or large amounts of mantle-derived basaltic magmas are necessary to transport advective heat in order to release it across the Moho (Aranovich et al. 2014)

melt extractability from migmatites cannot deliver the necessary volumes, as well. Thus, Aranovich et al. (2014) regard the intrusion of large amounts of mantle-derived basalt into the lowermost crust or their ponding below it as the major heat source and delivery of fluids and material for granite production.

Barker et al. (1992) described in detail what happens in the lowermost part of an accretionary prims, when basalts from the subducting plate are ascending. Given by the density contrast between greywackes and basalts, the latter would pool in the lowest parts of the prism. The basaltic magmas immediately quench upon contact with the much cooler greywackes and prevent mixing. On the other hand, the sediments undergo fast heating and melt diapirs develop.

Figure 5g of Laumonier et al. (2014) confirms this scenario from an experimental point of view. A greywacke-basalt system in the lower crust can only mix, when the viscosities of the two materials are identical, which is the case at a basalt fraction of 58% and a temperature of 1017 °C. Both conditions are probably not reached in general, because the greywacke melts tend to ascent before they reach 1000 °C.

Such greywacke-basalt systems could explain a couple of observations: (1) The banded amphibolites could represent deformed interminglings of basalts and felsic materials, which mutually penetrated each other but did not mix homogeneously. (2) There are no hybrid chemistries between paragneisses (metagreywackes) and amphibolites (metabasalts). Instead a clear miscibility gap (black stippled line with two arrowheads in Fig. 7) occurs between the two lithologies. (3) The possibility of heating greywackes near to their liquidus might represent a mechanism to lower their viscosity and allow the segregation of inclusions. This could produce very homogeneous S-type granitoids poor in enclaves.

In the A-B diagram of Fig. 10 the major granite production processes are visualized: (1) Basaltic magmas can evolve (a) by fractionated crystallization (e.g., Hbl fractionation) and (b) contamination by crustal rocks along the CAFEM field and produce high-temperature I-types like those of the Lachlan Fold Belt or the tonalite-diorite series of the Fusht Complex. The projection of continental margin calc-alkaline batholiths in the A-B diagram would show that the majority of the data plot in the metaluminous field, with the most acid varieties plotting in the low peraluminous field (Villaseca et al. 1998). (2) If greywackes and pelites melt, they first produce peraluminous to strongly peraluminous leucogranitoid melts and melanocratic restites. The former can be extracted to form pegmatites, aplites or smaller plutons. Higher degrees of melting (> 30%) produce diatexites, which can hold the solids and enclaves due to high viscosity (see discussion in Aranovich et al. 2014). Diapirism of such diatexites produces Ceneri gneisses or similar inclusion-rich S-types (Zurbriggen 2015) such as the Paradis gneiss and the similar Schmitzengneiss (Gotthard Nappe), the Mönchalp granite (Silvretta Nappe), the Winnebach granite and the similar Sulztaler, Inziger and Schlosskopf granites (Ötztal Nappe). If diatexites are further heated (due to continued intrusion and ponding of basalts) they liquefy until segregation of denser enclaves, resisters and xenoliths produces homogeneous S-types, which are poor in inclusions such as the Streifengneiss (Gotthard Nappe) or the Flüelagranitic gneisses (Silvretta Nappe). (3) Basalts and greywackes cannot mix due to viscosity contrasts at temperatures below 1000 °C (Laumonier et al. 2014). (4) Magma mixing on a large scale is only possible between granitoid magmas at temperatures of about 850 °C. This would explain the existence of low-temperature I-type granitoids, which bear characteristics of both, crustal-derived and mantle-derived material.

Fig. 10 A-B diagram (Debon and Le Fort 1988) with indicated sources of material and heat and magmatic processes (as listed with references in Table 3) for the genesis of peraluminous arc magmatism in subduction–accretion-complexes. For explanations see text

The processes of peraluminous magmatism are summarized in Table 3 and the block diagram of Fig. 11 visualizes the "zone of intermingling" at the base of a subduction–accretion complex. It shows an approximate 1:1 proportion of basalts and greywacke melts according to Barker et al. (1992) and Aranovich et al. (2014), who estimate that the melting of greywackes needs the heat input of an approximately equal amount of basalts. Hot basalts are intruding the lowermost metagreywackes as sills, dykes and stocks. The much cooler metagreywackes get heated and melt, while the basalts congeal and crystallize providing further crystallization heat. Viscosity contrast between the solidifying basalts and liquefying greywackes do not allow homogeneous mixing. As a result, only heat is transferred from the basalts to the greywacke melts, which intrude higher levels of the accretionary complex and get deformed to end as peraluminous orthogneisses in paragneiss country rocks. The role of crustal-scaled shear zones in transpressional orogens, such as subduction–accretion complexes, is crucial for the mobilization of magmas and interminglings to higher levels (see also D'Lemos et al. 1992). If these steep shear zones intersect a zone of peraluminous magma, then an orthogneiss sheet is produced and in case of eruption

rhyolites, as well. But if the steep shear zones intersect a "zone of intermingling", then a banded amphibolite is produced (see no. 2 in Fig. 11). Because amphibolites are denser, the probability to ascent is lower, therefore banded amphibolites are generally less abundant than orthogneisses. It can be assumed that such interminglings are too viscous for eruption and can reach higher crustal levels only by subsolidus shearing along deep reaching fault zones. This would also explain the rareness of mafic volcanics during the Ordovician (Heinisch 1981).

The paucity of mafic orthogneisses has two reasons: Firstly, basalts are significantly denser and tend to accumulate at the base of the accretionary prism (Barker et al. 1992). Secondly, the ponding basalts are overlain by a several km thick zone of migmatites (agmatites in the "zone of intermingling" with greywacke diatexites and metatexites on top), which are well ahead of ascending with regard to their higher position in the crust.

From the perspective of the above model of a "zone of intermingling", situated at the base of the subduction–accretion complex, banded amphibolites are mylonites of interminglings or other types of heterogeneous mixtures of different materials as illustrated in Fig. 12. Thus the "zone of intermingling" also acts as a trap for materials
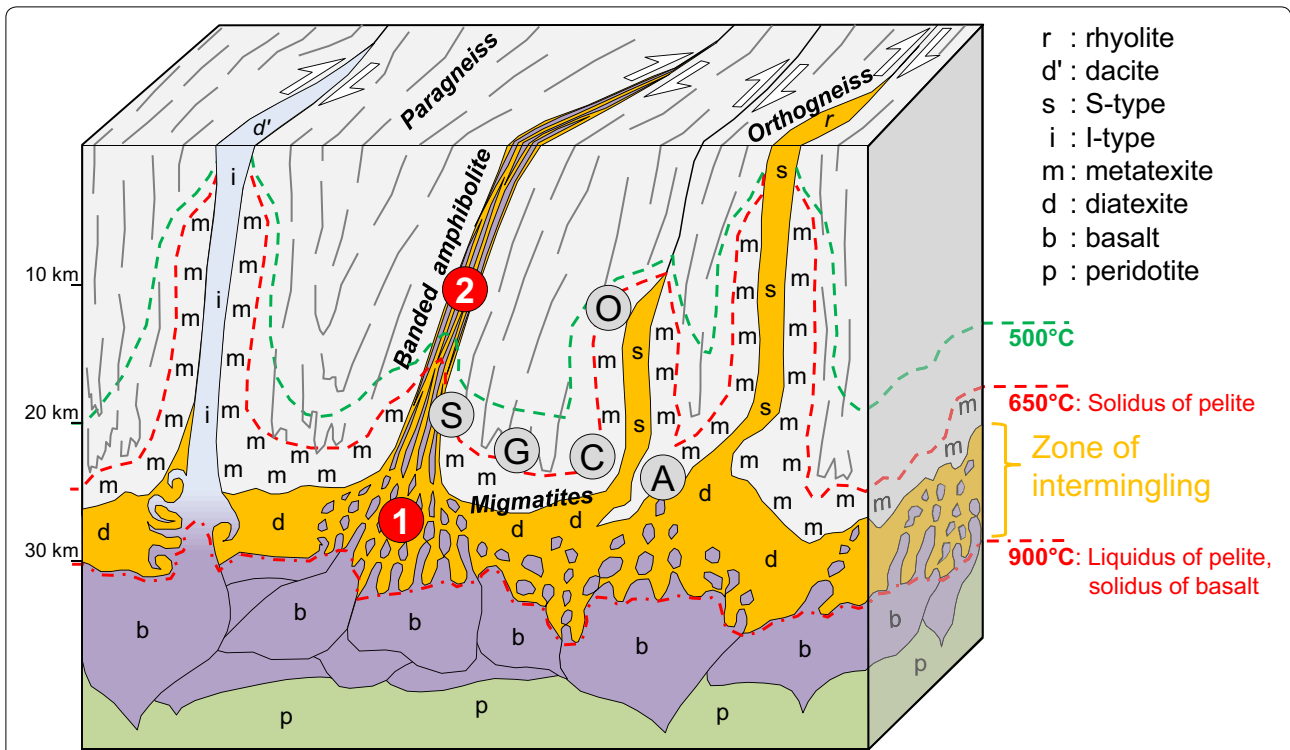
Fig. 11 Schematic block diagram of intermingling zone at the Moho. It visualizes the generation of the four main lithologies (para- and orthogneisses, migmatites and banded amphibolites) during the cratonization of a subduction–accretion complex (Zurbriggen 2017). Abbreviations: 1: first production step of banded amphibolites by intermingling, 2: second production step of banded amphibolites by shearing, O: Ötztal Nappe, S: Silvretta Nappe, G: Gotthard Nappe, C: Strona-Ceneri Zone, A: Aar Massif. The units are located according to their individual lithological characteristics. For further explanations see text
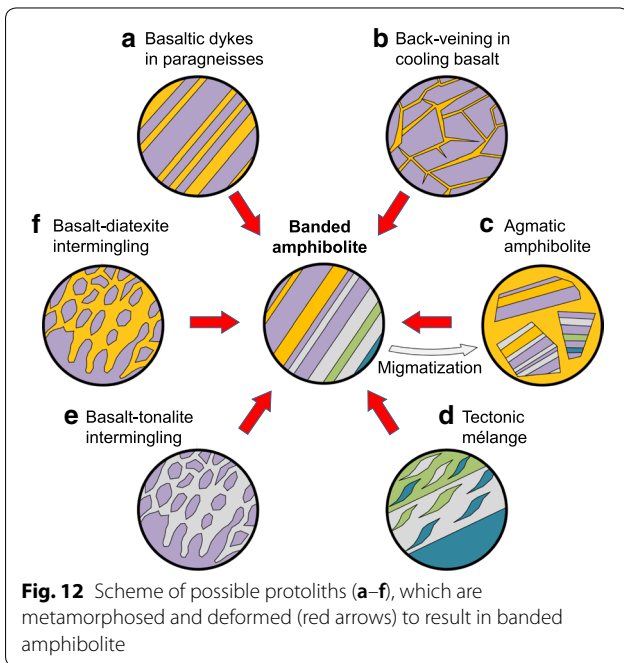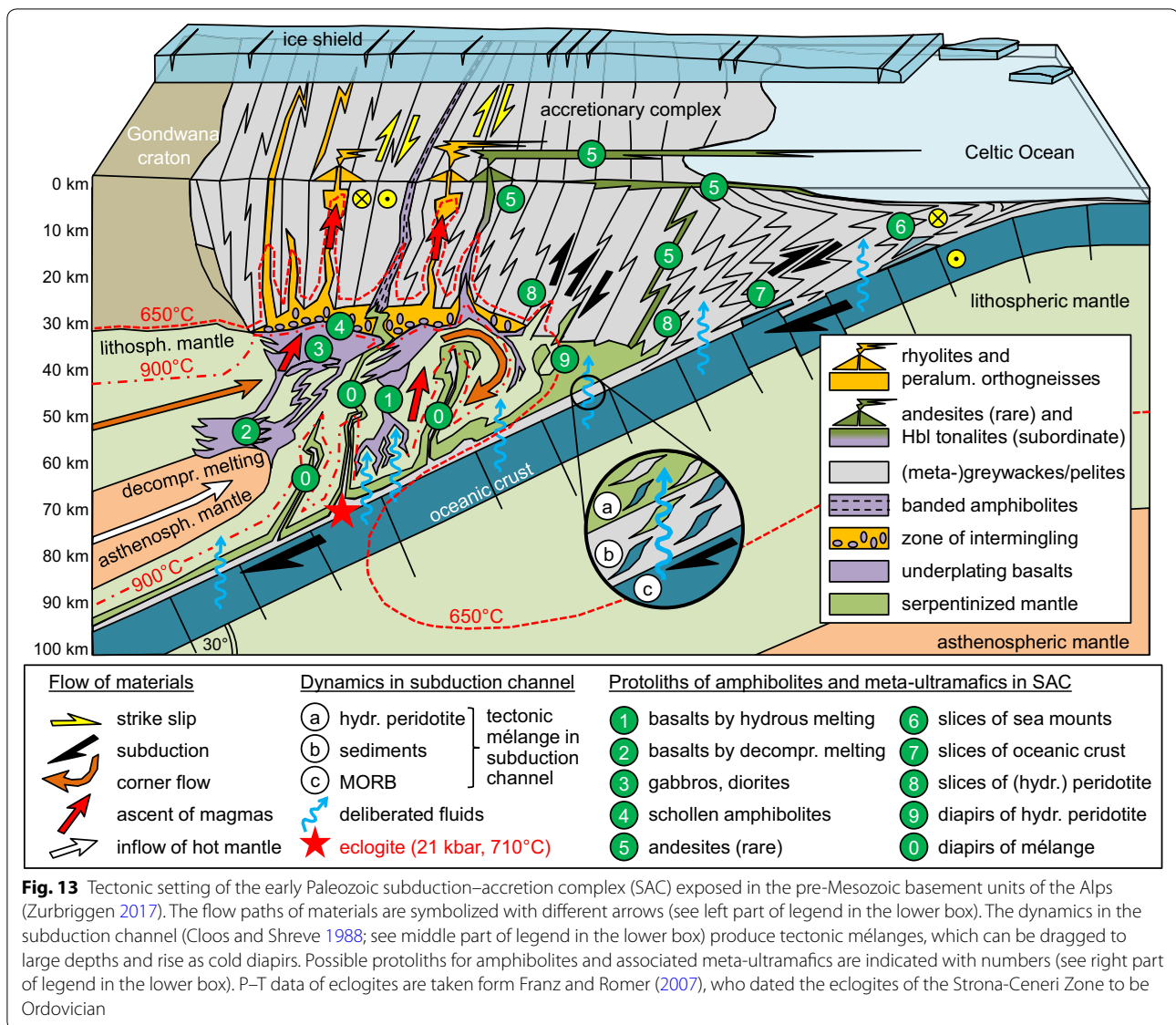

Fig. 12 Scheme of possible protoliths (**a**–**f**), which are metamorphosed and deformed (red arrows) to result in banded amphibolite

such as tectonic mélanges which can ascent as cold diapirs (Timm et al. 2014; Cruz-Uribe et al. 2018) and peridotites from the mantle wedge, which are sheared into the accretionary complex.

6.2 Discussion of the tectonic setting and the role of banded amphibolite formations

Figure 13 is an illustration of the many simultaneous processes during the cratonization of a subduction–accretion complex. "Cratonization", a process described by Crook (1980), means the transition from a cold accretionary prism to a hot accretionary complex during peraluminous magmatism (Zurbriggen 2017) to result in a stable cratonic crust. The magmatism inverts the crust by the ascent of the magmas from the "zone of intermingling" along shear zones to emplace at higher levels of the accretionary complex as orthogneisses or extrude as rhyolites. As a result, new crust is formed at the periphery of the growing continent. The material for this new crust is mainly of crustal origin (c. 97% in case of the Strona-Ceneri Zone; Zurbriggen 2015). Thus, the cratonization

Fig. 13 Tectonic setting of the early Paleozoic subduction–accretion complex (SAC) exposed in the pre-Mesozoic basement units of the Alps (Zurbriggen 2017). The flow paths of materials are symbolized with different arrows (see left part of legend in the lower box). The dynamics in the subduction channel (Cloos and Shreve 1988; see middle part of legend in the lower box) produce tectonic mélanges, which can be dragged to large depths and rise as cold diapirs. Possible protoliths for amphibolites and associated meta-ultramafics are indicated with numbers (see right part of legend in the lower box). P–T data of eclogites are taken form Franz and Romer (2007), who dated the eclogites of the Strona-Ceneri Zone to be Ordovician

of subduction–accretion complexes is a recycling of terrigeneous sediments. However, the heat for the cratonization is delivered by mantle-derived basalts intruding the base of the accreted sediments, as described by Barker et al. (1992) for the forearc granitoids in the accretionary prism of the Gulf of Alaska.

With growing width of a subduction–accretion complex the lithospheric mantle underneath is thinned and asthenospheric mantle can flow upwards. Therefore both, fluid-induced melting of lithospheric mantle and decompression-melting of upflowing asthenospheric mantle produce calc-alkaline and tholeiitic basalts, respectively, which is reflected in the chemistry of the amphibolites (Fig. 8).

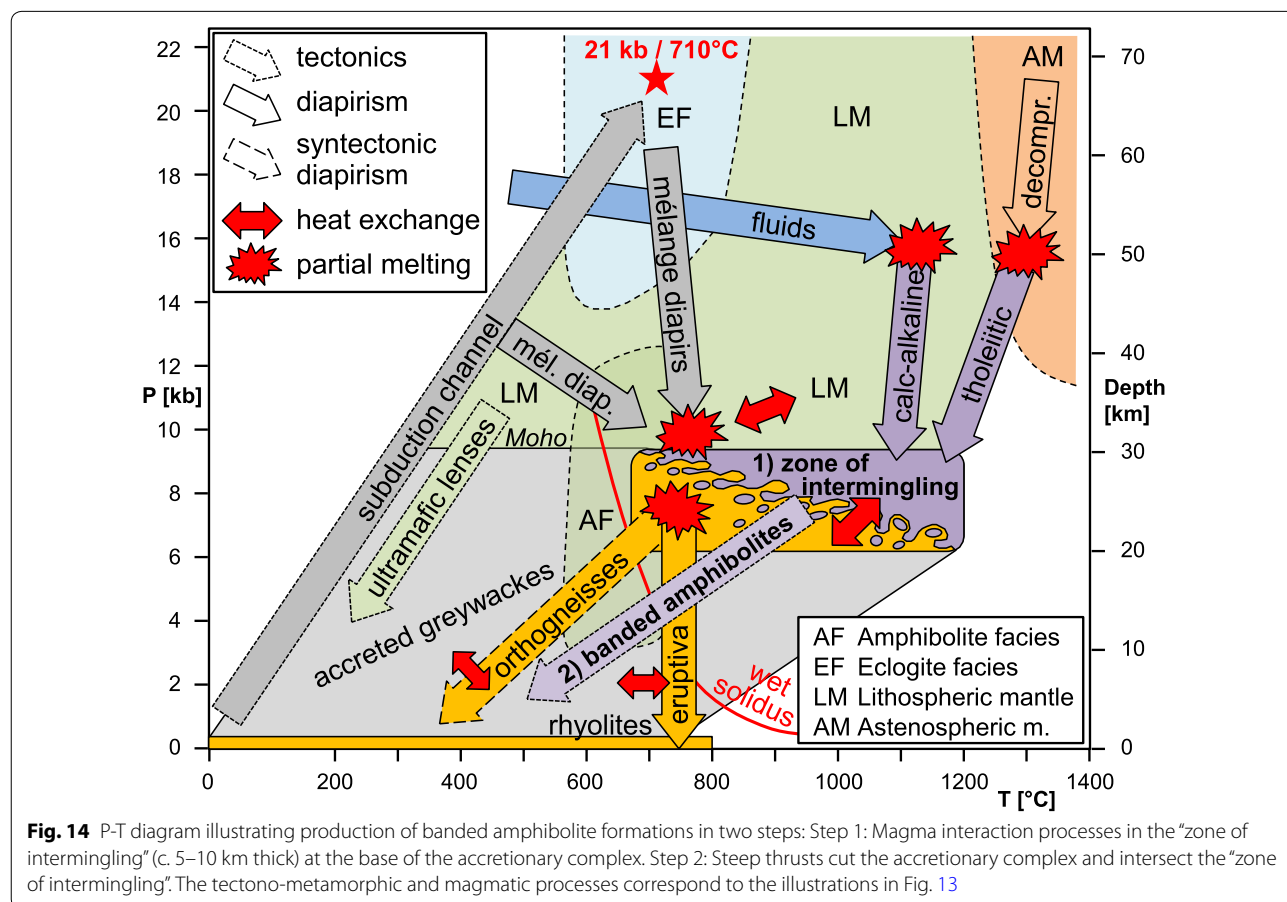The "zone of intermingling" plays three major roles:

1. It acts as a collector for a large variety of lithologies, which reflect the many dynamics in the mantle wedge. The deliberation of fluids from the subducting plate induces melting of the overlying mantle wedge (flux melting) and the production of calc-alkaline basalts. Upflowing hot mantle produces tholeiitic basalts by decompression melting. Cagnioncle et al. (2007; see their Fig. 13) mention that in subduction zones both, flux-derived melts and decompression melts can be generated in order to explain the compositional range. In sum, large quantities of different basalts ascent, underplate and intrude the base of the accreted greywackes, initiate regional anatexis and cause peraluminous magmatism. Due to (a) the downwards flow of the subducting plate carry-

ing mélanges to eclogitic depths and (b) the upward flow of mantle and magmas, the isotherms form vertical "fingers" in the mantle wedge and in the prism (Fig. 13). Along these "fingers" materials and heat are rapidly transported to higher levels. This converts the initially cold prism into a hot accretionary complex with peraluminous magmatism (see Fig. 2 in Zurbriggen 2017). However, the upward flow of mantle-derived materials generally stops in the "zone of intermingling", and the peraluminous magmas start to rise from there and transport heat further up and initiate migmatization at higher levels. There, mixing and mingling between felsic magmas and migmatites can cause the formation of felsic MASH zones as described by Schwindinger and Weinberg (2017). This explains the stepwise heat transfer form basalts to deep-crustal metagreywackes to generate peraluminous granites, and from the latter to migmatites in higher crustal levels. However, the primary heat is provided by the mantle, but the mantel-derived materials generally remain in the lowermost crust or below the Moho.

2. The "zone of intermingling" acts as a heat exchanger, where the hot basalts transfer their heat to the melting greywackes. The efficiency of heat exchangers is dependent on the differential temperature, the thermal conductivity and the interfacial area. The latter is strongly increased by dyke intrusions and heterogeneous intermingling. These mechanism result in intercalations of banded amphibolites with migmatites (Fig. 4).

3. The "zone of intermingling" acts as a granite kitchen, the production site for peraluminous magmas. This scenario is supported by contemporaneous gabbros in all these terranes (Von Raumer et al. 2013).

The numbers in Fig. 13 indicate possible protoliths for amphibolites and meta-ultramafics. Andesitic volcanics are indicated as a possibility, but according to Heinisch (1981), andesites are rare compared to the large volumes of rhyolites and dacites.

Another aspect of such gneiss terranes are the many transitional species (so called "Mischgneise" as discussed in Zurbriggen 1996, p. 33) between para- and orthogneisses and banded amphibolites, which locally can be

Fig. 14 P-T diagram illustrating production of banded amphibolite formations in two steps: Step 1: Magma interaction processes in the "zone of intermingling" (c. 5–10 km thick) at the base of the accretionary complex. Step 2: Steep thrusts cut the accretionary complex and intersect the "zone of intermingling". The tectono-metamorphic and magmatic processes correspond to the illustrations in Fig. 13

feldspathized. The occurrence of K-feldspar porphyroblasts is discussed in the context of fluid and/or melt infiltration by Pinarelli et al. (2008). These mechanisms are very probable because subduction brings large quantities of fluids into the mantle wedge and the overlying accretionary complex, and large volumes of melts are generated in the mantle and in the accretionary complex, which are ascending to higher levels and even extrude.

The tectono-metamorphic and magmatic processes of a cratonizing subduction–accretion complex can also be visualized in a P–T diagram (Fig. 14). In the center of the P–T-t evolution is the "zone of intermingling", wherein the protoliths of the banded amphibolites (the first production step as denoted with no. 1 in Figs. 11 and 14) occurs. Note the many flow paths of different materials into the "zone of intermingling", which generate the large variety of rocks, fluids and magmas. Important to mention is the mechanism for the exhumation of eclogites. They ascent as fragments in cold mélange diapirs through the mantle wedge. If they remain in the "zone of intermingling" they convert to granulites or amphibolites. But if the residence time is short, because they are readily sucked and sheared into a crustal shear zone, eclogites can emplace in the accretionary complex. However, the majority of the dense eclogites will be subducted, but enclosed in mélange diapirs and intermingled magmas they can ascent fast enough and survive as such.

The second production step of banded amphibolites occurs by mobilization of intermingled magmas along deep-reaching fault zones (see no. 2 in Figs. 11 and 14). This mechanism would also explain why in the field the banded amphibolites are linearly arranged and associated with orthogneisses, migmatites, (meta-)gabbros, (meta-) eclogites and (meta-)ultramafics.

In contrast to peraluminous rocks (metapelites, metagreywackes, migmatites and orthogneisses), which have a similar density and are more evenly distributed across the crust, the banded amphibolite formations vary strongly in percentages, because of their relative high density. This explains their variable occurrence in different regions by a factor of 10, ranging from c. 2 area% in the Strona-Ceneri Zone to 22 area% in the Silvretta Nappe. Also their association with ultramafics and their degree of mylonitization can vary strongly, because of the heterogeneous distribution of these rocks at depth and below the accretionary prism, and because each banded amphibolite is the result of an individual shear zone.

6.3 Discussion of the early Paleozoic circum-Gondwanan setting

A comparison with many studies from peri-Gondwanan terranes (Table 4) indicates that peraluminous magmatism was a global phenomenon in early Paleozoic times.

This global feature was the result of a combination of two factors, both of which were unique for the post-Panafrican era.

1. The assembly of Gondwana was associated with the closure of the oceans between cratons and a jump of subductions to the periphery of the supercontinent as described for East-Gondwana by Foden et al. (2006). Therefore, Gondwana was framed at the beginning of the Paleozoic by two major subduction systems (e.g., Rino et al. 2008), the Avalonian-Cadomian one facing the Celtic Ocean, and the Ross-Delamerian one facing the Paleo-Pacific Ocean (e.g., Zurbriggen 2017).
2. The erosion of the Transgondwanan Supermountain delivered an estimated volume of sediment of > 100 Mkm³, which corresponds to a 10 km thick layer covering the entire USA (Squire et al. 2006). These sediments were transported by river systems and ice shields into the trenches of the circum-Gondwanan subduction systems and caused the formation of fast-growing subduction–accretion complexes (Fig. 15).

The purpose of Table 4 is to show that peraluminous magmatism is a circum-Gondwanan phenomenon during the entire early Paleozoic. The different magmatic events are related to regionally different orogenies, but I doubt the general relationship of peraluminous magmatism to rifting or collisional settings for reasons raised in the methodological part (Sect. 2.2), and because greywackes are a basic element of active margins (Barker et al. 1992; Zurbriggen 2017). The data compilation of Table 4 should lead the reader into the direction of looking at peraluminous arcs from the perspective of cratonizing subduction–accretion complexes, a hitherto poorly recognized circum-Gondwanan tectonic setting in early Paleozoic times.

Regarding the provenance of the protoliths of the pre-Variscan paragneisses in the Alps the following can be said. According to Fig. 7 of Pinarelli et al. (2008) the augen gneisses of the Strona-Ceneri Zone have protolith ages indicating the Cadomian and Grenvillian events. The same age memory is shown by Austroalpine paragneisses (see Fig. 8d of Siegesmund et al. 2018) indicating the Arabian-Nubian Shield (the host of the Fusht Complex) as provenance. This is also supported by reconstructions of Avigad et al. (2017).

Figure 15 is a compilation of the peri-Gondwanan terranes with early Paleozoic peraluminous magmatism indicating the anatexis of metasediments within the setting of cratonizing subduction–accretion complexes.

Foster and Goscombe (2013) mention that 20% of the outcrop area of the Lachlan Fold Belt are composed of granitoids and half of them are S-types. About 70% of all

Table 4 Compilation of references for early Paleozoic peraluminous magmatism in peri-Gondwanan basement units

Peri-Gondwanan basement unit	Magmatism [Ma]	Chappell and White (2001)	Foster and Goscombe (2013)	Foden et al. (2006)	Schwartz et al. (2008)	Goodge (2007)	Farina et al. (2012)	Rossi et al. (2002)	Fernández et al. (2008)	Díaz-Alvarado et al. (2016)	Ballèvre et al. (2012)	Pouclet et al. (2016)	Zurbriggen (2015)	Villaseca et al. (2016)	Zurbriggen (2017)	Garcia-Arias et al. (2018)	Von Raumer et al. (2013)	Stephan et al. (2019)	Casas and Murphy (2018)	Siebel et al. (1997)	Linnemann (2007)	Balintoni et al. (2011, 2013)	Cruciani et al. (2019)	Korálay et a. (2012)	Rossetti et al. (2015)	Hu et al. (2015)	Lin et al. (2013)	Osterle et al. (2019)
Lachlan Fold Belt (SE Australia)	430–370																											
Delamerian (SE Australia)	522–478																											
Ross orogen (Antarctica)	550–480																											
Saldanian orogen (South Africa)	550–510																											
Pampean orogen (Argentina)	555–515																											
Iberian Variscan belt (Spain)	496–457																											
South Armorican and Occitan domains of the Variscan Belt (France)	494–473																											
Strona-Ceneri Zone and other pre-Mesozoic basement units of the Alps	510–430																											
Saxothuringian zone (Germany)	480																											
Bohemian Massif (Germany)	560–540																											
Carpathians (Romania)	495–460																											
Sicily (Italy)	492–440																											
Menderes Massif (Turkey)	550–530																											
Kuh-e-Sarhangi region (Iran)	575–535																											
South Qiangtang terrane (North Tibet)	486–480																											
Sibumasu terrane and Lan Sang gneiss complex (Thailand)	500–470																											

Anatexis related granitoids, S-type granitoids, or augen gneisses are included as well. Dark grey fields: comparative studies; light grey fields: studies of specific regions
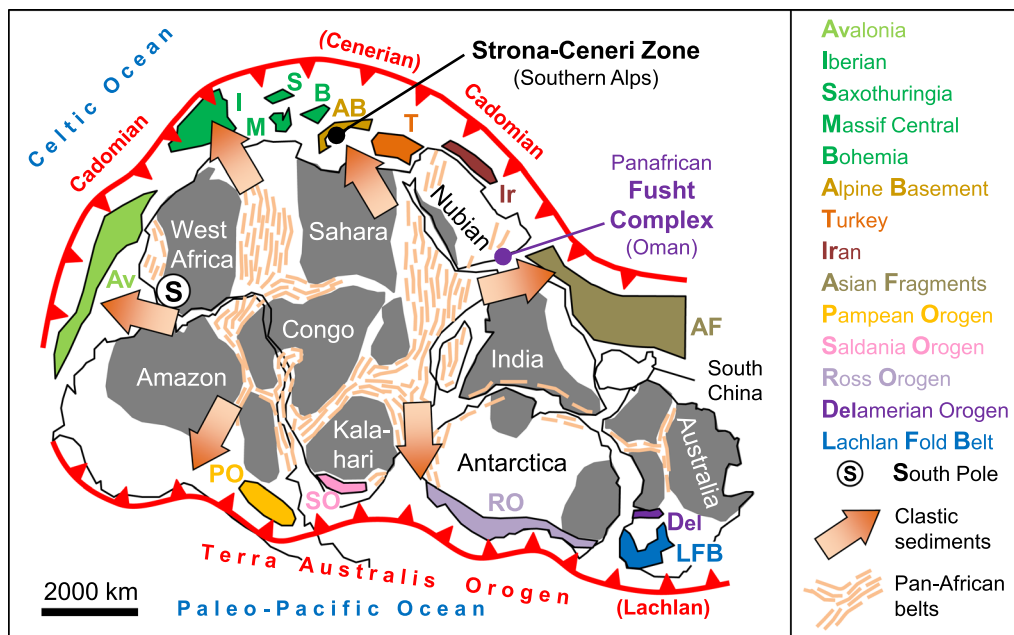
Fig. 15 Map of Gondwana in the period of 550–500 Ma with indicated Paleozoic orogenic sutures, along which material (mainly detritus) was accreted and recycled by the cratonization of subduction–accretion complexes (see Table 4). The Cenerian (490–440 Ma) and Lachlan (430–370 Ma) orogenies occurred later and are therefore in brackets. The Strona-Ceneri Zone is part of the Alpine Basement (AB). The Fusht Complex in southern Oman (790 Ma) belongs to an older Pan-African arc system (drawn after Kröner and Stern 2004; Schmitt et al. 2004; Linnemann 2007; Fernández et al. 2008; Foster and Gray 2008; Schwartz et al. 2008; Ustaömer et al. 2009; Torsvik and Cocks 2011; Koralay et al. 2012; Foster and Goscombe 2013; Lin et al. 2013; Hu et al. 2015; Santosh et al. 2014; Rossetti et al. 2015; Shafaii Moghadam et al. 2015; Villaseca et al. 2016; Avigad et al. 2017; Li et al. 2017; and Zurbriggen 2017. Pre-Variscan basements of the Alps, including the Strona-Ceneri Zone (SCZ), were located according to Von Raumer et al. 2015)

Lachlan granitoids are peraluminous (Chappell and White 2001). Schwartz et al. (2008) have compared the early Paleozoic orogenic belts of the Terra Australis Orogen (Fig. 15) namely the Pampean (Argentina), the Saldanian (South Africa; see also Farina et al. 2012), the Ross (Transantarctica; see also Goodge 2007), and the Delamerian (Australia; see also Foden et al. 2006). With the probable exception of the Ross orogen, the common feature of these belts is an arc-related magmatism including strongly peraluminous suites. Schwartz et al. (2008) focused on the Pampean orogen, more specifically on the Eastern Sierreas Pampeanas, which is divided into an Eastern Calc-Alkaline Arc Belt (555–525 Ma) and a western Metasedimentary Belt hosting migmatites and peraluminous granitoids (525–515 Ma). The boundary in between corresponds to the I-S line of Rossi et al. (2002), who studied the Ordovician Capillitas batholith about 500 km further to the NNW. The Capillitas batholith is just west of this I-S line and resembles to the Cooma granodiorite, the type locality of Chappell and White's S-type granitoid in the Lachlan Fold Belt. From the Capillitas batholith northwards Fernández et al. (2008) studied the Cambro-Ordovician peraluminous magmatism of the Eastern Puna Eruptive Belt (Argentina) and found similarities in age, volumes and chemistry to the Ollo de Sapo formation of Iberia (Spain). Villaseca et al. (2016) regarded the Ollo de Sapo formation as a part of a transeuropean Cambro-Ordovician mainly peraluminous arc system, which corresponds to the Cenerian belt of Zurbriggen (2017).

Evidence for similar early Paleozoic anatexis and peraluminous magmatism is also reported from the Fichtelgebirge in the Saxothuringian Belt (Siebel et al. 1997), the Bohemian Massif (Linnemann et al. 2014) and the Romanian Carpathians (Balintoni and Balica 2013; Balintoni et al. 2011, 2014). The broadest comparison along northern Gondwana is done by Stephan et al. (2019; see Table 4) with reference to the Cenerian orogeny along the eastern part of the Peri-Gondwanan shelf.

In Turkey (Ustaömer et al. 2009; Koralay et al. 2012) and Iran (Shafaii Moghadam et al. 2015; Rossetti et al. 2015) 550–530 Ma old orthogneisses indicate that the late Cadomian arc system (Linnemann et al. 2014) has continued eastwards over Turkey, Iran to Asia (Kröner and Stern 2004). Hu et al. (2015) describe early Ordovician S-type magmatism in Tibet. Lin et al. (2013) and Österle et al. (2019) identified 470–500 Ma old orthogneisses in the Sibumasu terrane and the Lan Sang gneiss complex of Thailand. These studies connect the early Paleozoic

European-Asian arc system with the Terra Australis Orogen to one circum-Gondwanan subduction system.

The works of Ustaömer et al. (2009) and Shafaii Moghadam et al. (2015) point to a late Cadomian I-type magmatism in Turkey and Iran, respectively. This is in line with a general change from an I-type dominance during the Cadomian orogeny (Andean type continental arcs) to a S-type dominance during the Cenerian orogeny (Alaskan type subduction–accretion complexes) as shown in Fig. 6 of Zurbriggen (2017).

However, the dominance of I-type or S-type magmatism is a function of the subduction rate and sediment flux. If subduction rate is high and/or the sediment flux is low, the magmatism becomes increasingly metaluminous, because the primary basalts are not rapidly cooled by melting metasediments, and diorite-tonalite series evolve by fractional crystallization. It becomes evident, that the I-S lines of Chappell et al. (1988), Rossi et al. (2002) and Zurbriggen (1996) for the Lachlan Fold Belt (Australia), the Pampean ranges (Argentina) and the Strona-Ceneri Zone (Southern Alps), respectively, mark borders, where the amount of transferred material at the Moho changes. If only heat transfers and no basaltic material, then a pure peraluminous magmatism develops. If basaltic material is transferred as well, then a mixed metaluminous/peraluminous or even e pure metaluminous magmatism develops. In the evolution of a cratonizing subduction–accretion complex (SAC) a change in the angle or rate of subduction or a change in the rate of sediment flux from the hinterland can cause a shift from peraluminous towards a metaluminous magmatism or vice versa, generating I-S lines.

The circum-Gondwanan arrangement of subduction zones caused transpressive tectonics, which play a key role in the emplacement of magmas as indicated in Fig. 11. In fact, both, Linnemann et al. (2014) and Schwartz et al. (2008) indicate transpressive tectonics for the Cadomian and Terra Australis Orogen, respectively.

7 Conclusions

Following conclusions can be made:

1. The orthogneisses, paragneisses, migmatites and amphibolites of the pre-Variscan basement units in the Alps indicate a common history during the Cenerian orogeny in early Paleozoic times.
2. The Ordovician orthogneisses represent peraluminous to strongly peraluminous metagranitoids, which were generated mainly by anatexis of metasediments with minor material input from the mantle. They can be grouped into subordinate Hbl-bearing orthogneisses (type 1), most abundant homogeneous peraluminous orthogneisses and augen gneisses (type 2), and ferrosilicic inclusion-rich S-types (e.g., Ceneri gneiss-like lithologies). The latter generated by the total-melting of greywackes (type 3).
3. Volumetric estimations indicate that the lowermost 6.25–7.5 km of a 25–30 km thick accretionary complex must melt to provide the necessary quantity of peraluminous orthogneisses and migmatites.
4. The required heat must be provided by a similar amount of mantle-derived basalts. They can have calc-alkaline or tholeiitic signatures, because both types of partial melting of mantle can occur underneath large subduction–accretion complexes, such as fluid induced melting related to the subducting plate and decompression melting of ascending asthenospheric mantle.
5. The basalts quench in contact with the relatively cool metagreywackes and homogeneous mixing cannot occur due to viscosity contrast between solidifying basalts and liquefying greywacke-melts. Therefore mainly heat is transferred from basalts to greywackes in the "zone of intermingling" and due to their higher density the mafics tend to sink and remain at depth, while the peraluminous magmas ascent to become orthogneisses.
6. Thereby, transpressive shear zones play an important role for the emplacement mechanism causing the sheet-like geometry of the orthogneisses.
7. Intermingling of basaltic magmas and greywacke melts create the protoliths of the banded amphibolites. If they are sheared into the accretionary complex (similarly as the orthogneisses) banded amphibolites are generated.
8. The "zone of intermingling" is also a trap for diapirs of serpentinized peridotite and cold subduction mélanges. The latter can carry eclogitic fragments. Therefore, banded amphibolites (mylonitized interminglings) are locally associated or linearly arranged with trails of (meta-)eclogitic and (meta-)ultramafic lenses. This explains the large lithological variety in banded amphibolite formations, which can be observed in all pre-Mesozoic gneiss terranes of the Alps.
9. The banded amphibolites represent mafic complexes containing the primary basaltic melts, which initiated anatexis followed by felsic magmatism. But because the basalts mainly provide the heat for anatexis without a substancial material input, the magmatism is peraluminous to strongly peraluminous and mafic microgranular enclaves and mafic endmembers are rare.
10. Peraluminous magmatism is a global peri-Gondwanan phenomenon in early Paleozoic times. It is caused by the extraordinary sediment flux (from

eroding Pan-African belts) into a circum-Gond-wanan subduction system. This resulted in the formation of subduction–accretion complexes, which cratonized during peraluminous magmatism.

11. The dynamics in the mantle below subduction–accretion complexes are very fast. This is due to the (i) deliberation of fluids from the subducting plate, (ii) ascending diapirs of serpentinized peridotite and cold mélanges containing eclogites, (iii) intensive partial melting of lithospheric and asthenospheric mantle providing large volumes of calc-alkaline and tholeiitc basalts, respectively.

12. Thus, the dynamics in hot accretionary complexes with peraluminous magmatism are rooted in the dynamics of the mantle underneath.

Authors' contributions
The author read and approved the final manuscript.

Authors' information
This manuscript provides new field observations and a reinterpretation of existing geochemical data in the context of a new model for the Ordovician orogeny in the Alps. This new model was published by the same author in 2015 and 2017 (see reference list).

Availability of data and materials
There is no unpublished data contained in the manuscript and all data is carefully referred.

Ethics approval and consent to participate
Not applicable for this section.

Consent for publication
Not applicable.

Competing interests
The author declares that he has no competing interests.

Author details
[1] Institute of Geological Sciences, Bern, Switzerland. [2] Neuenkirch, Switzerland.

References
Abrecht, J. (1994). Geologic units of the Aar massif and their pre-Alpine rock associations: a critical review. *Schweizerische Mineralogische und Petrographische Mitteilungen, 74,* 5–27.

Aranovich, L. Y., Makhluf, A. R., Manning, C. E., & Newton, R. C. (2014). Dehydration melting and the relationship between granites and granulites. *Precambrian Research, 253,* 26–37.

Avigad, D., Morag, N., Abbo, A., & Gerdes, A. (2017). Detrital rutile U-Pb perspective on the origin of the great Cambro-Ordovician sandstone of North Gondwana and its linkage to orogeny. *Gondwana Research, 51,* 17–29.

Bächlin, R. (1937). Geologie und Petrographie des M. Tamaro-Gebietes (südliches Tessin). *Schweizerische Mineralogische und Petrographische Mitteilungen, 17,* 1–79.

Balintoni, I., & Balica, C. (2013). Carpathian peri-Gondwanan terranes in the East Carpathians (Romania): A testimony of an Ordovician, North-African orogeny. *Gondwana Research, 23,* 1053–1070.

Balintoni, I., Balica, C., Ducea, M. N., & Hann, H.-P. (2014). Peri-Gondwanan terranes in the Romanian Carpathians: A review of their spatial distribution, origin, provenance, and evolution. *Geoscience Frontiers, 5*(3), 395–411.

Balintoni, I., Balica, C., & Hann, H. P. (2011). About a peri-Gondwanan—North African enlarged acceptance of the Caledonian orogeny. *Studia UBB, Geologia, 56*(1), 29–32.

Ballèvre, M., Fourcade, S., Capdevila, R., Peucat, J.-J., Cocherie, A., & Fanning, C. M. (2012). Geochronology and geochemistry of Ordovician felsic volcanism in the Southern Armorican Massif (Variscan belt, France): Implications for the breakup of Gondwana. *Gondwana Research, 21,* 1019–1036.

Barker, F., Farmer, G. L., Ayuso, R. A., Plafker, G., & Lull, J. S. (1992). The 50 Ma granodiorite of the Eastern Gulf of Alaska: melting in an accretionary prism in the forearc. *Journal of Geophysical Research, 97*(B5), 6757–6778.

Berger, A., Mercolli, I., Herwegh, M., & Gnos, E. (2016). Geological map of the Aar Massif, Tavetsch and Gotthard Nappes. 1:100'000, No. 129, *Swiss Geological Survey.*

Boriani, A., Burlini, L., & Sacchi, R. (1990). The Cossato–Mergozzo–Brissago Line and the Pogallo Line (Southern Alps, Northern Italy) and their relationships with the late-Hercynian magmatic and metamorphic events. *Tectonophysics, 182,* 91–102.

Boriani, A., Giobbi Origoni, E., & Pinarelli, L. (1995). Paleozoic evolution of southern Alpine crust (northern Italy) as indicated by contrasting granitoid suites. *Lithos, 35,* 47–63.

Buletti, M. (1983). Zur Geochemie und Entstehungsgeschichte der Granat-Amphibolite des Gambarognogebietes, Ticino, Südalpen. *Schweizerische Mineralogische und Petrographische Mitteilungen, 63,* 233–247.

Bussien, D., Bussy, F., Magna, T., & Masson, H. (2011). Timing of Paleozoic magmatism in the Maggia and Sambuco nappes and paleogeographic implications (Central Lepontine Alps). *Swiss Journal of Geosciences, 104,* 1–29.

Cagnioncle, A.-M., Parmentier, E. M., & Elkins-Tanton, L. T. (2007). Effect of solid flow above a subducting slab on water distribution and melting at convergent plate boundaries. *Journal of Geophysical Research, 112*(B09402), 1–19. https://doi.org/10.1029/2007JB004934.

Casas, J. M., & Murphy, J. B. (2018). Unfolding the arc: The use of pre-orogenic constraints to assess the evolution of the Variscan belt in Western Europe. *Tectonophysics, 736,* 47–61.

Castro, A., García-Casco, A., Fernández, C., Corretgé, L. G., Moreno-Ventas, I., Gerya, T., et al. (2009). Ordovician ferrosilicic magmas: Experimental evidence for ultrahigh temperatures affecting a metagreywacke source. *Gondwana Research, 16,* 622–632.

Chappell, B. W., & White, A. J. R. (1974). Two contrasting granite types. *Pacific Geology, 8,* 173–174.

Chappell, B. W., & White, A. J. R. (1992). I- and S-type granites in the Lachlan fold belt. *Transactions of the Royal Society of Edinburgh, Earth Sciences, 83,* 1–26.

Chappell, B. W., & White, A. J. R. (2001). Two contrasting granite types: 25 years later. *Australian Journal of Earth Sciences, 48,* 489–499.

Chappell, B. W., White, A. J. R., & Hine, R. (1988). Granite provinces and basement terranes in the Lachlan Fold Belt, southeastern Australia. *Australian Journal of Earth Sciences, 35,* 505–521.

Chappell, B. W., White, A. J. R., Williams, S., & Wyborn, D. (2004). Low- and high-temperature granites. *Transactions of the Royal Society of Edinburgh, Earth Sciences, 95,* 125–140.

Cloos, M., & Shreve, R. L. (1988). Subduction-channel model of prism accretion, melange formation, sediment subduction, and subduction erosion at convergent plate margins: 1. Background and description. *Pageoph, 128*(3/4), 455–500.

Crook, K. A. W. (1980). Fore-arc evolution and continental growth: a general model. *Journal of Structural Geology, 2*(3), 289–303.

Cruciani, G., Fancello, D., Franceschelli, M., & Musumeci, G. (2019). Geochemistry of the Monte Filau orthogneiss (SW Sardinia, Italy): insight into the geodynamic setting of Ordovician felsic magmatism in the N/NE Gondwana margin. *Italian Journal of Geosciences, 138,* 136–152. https://doi.org/10.3301/IJG.2018.32.

Cruz-Uribe, A. M., Marschall, H. R., Gaetani, G. A., & Le Roux, V. (2018). Generation of alkaline magmas in subduction zones by partial melting of mélange diapirs—An experimental study. *Geology, 46*(4), 343–346.

D'Lemos, R. S., Brown, M., & Strachan, R. A. (1992). Granite magma generation, ascent and emplacement within a transpressive orogen. *Journal of the Geological Society, London, 149,* 487–490.

Debon, F., & Le Fort, P. (1988). A cationic classification of common plutonic rocks and their magmatic associations: principles, method, applications. *Bulletin de Minéralogie, 111,* 493–510.

Díaz-Alvarado, J., Fernández, C., Chichorro, M., Castro, A., & Pereira, M. F. (2016). Tracing the Cambro-Ordovician ferrosilicic to calc-alkaline magmatic association in Iberia by in situ U-Pb SHRIMP zircon geochronology (Gredos massif, Spanish Central System batholith). *Tectonophysics, 681,* 95–110.

Egger, H., Krenmayr, H.G., Mandl, G.W., Matura, A., Nowotny, A., Pascher, G., Pestal, G., Pistotnik, J., Rockenschaub, M., & Schnabel, W. (1999). Geologische Übersichtskarte der Republik Österreich. Geologische Bundesanstalt, Wien, see also Webpage of Multithematische geologische Karte von Österreich 1:1.000.000, Geologische Bundesanstalt, FastAccess, Multi-Thematic Geological Map.

Farina, F., Stevens, G., & Villaros, A. (2012). Multi-batch, incremental assembly of a dynamic magma chamber: the case of the Peninsula pluton granite (Cape Granite Suite, South Africa). *Mineralogy and Petrology.* https://doi.org/10.1007/s00710-012-0224-8.

Fernández, C., Becchio, R., Castro, A., Viramonte, J. M., Moreno-Ventas, I., & Corretgé, L. G. (2008). Massive generation of a typical ferrosilicic magmas along the Gondwana active margin: Implications for cold plumes and back-arc magma generation. *Gondwana Research, 14,* 451–473.

Foden, J., Elburg, M. A., Dougherty-Page, J., & Burtt, A. (2006). The timing and duration of the Delamerian orogeny: Correlation with the Ross orogen and implications for Gondwana assembly. *The Journal of Geology, 114,* 189–210.

Foster, D. A., & Goscombe, B. D. (2013). Continental growth and recycling in convergent orogens with large turbidite fans on oceanic crust. *Geosciences, 3,* 354–388.

Foster, D.A., & Gray, D.R. (2008). Paleozoic crustal growth, structure, strain rate, and metallogeny in the Lachlan orogen, eastern Australia. In J.E. Spencer, & S.R. Titley SR (Eds.), *Ores and orogenesis: Circum-Pacific tectonics, geologic evolution, and ore deposits* (Vol. 22, pp. 213–225). Arizona Geological Society Digest.

Franz, L., & Romer, R. L. (2007). Caledonian high-pressure metamorphism in the Strona-Ceneri Zone (Southern Alps of southern Switzerland and northern Italy). *Swiss Journal of Geosciences, 100*(3), 457–467.

Frey, M., Hunziker, J. C., Frank, W., Bocquet, J., Dal Piaz, G. V., Jäger, E., et al. (1974). Alpine metamorphism of pelitic and marly rocks of the central Alps. *Schweizerische Mineralogische und Petrographische Mitteilungen, 54,* 489–506.

García-Arias, M., Díez-Montes, A., Villaseca, C., & Blanco-Quintero, I. F. (2018). The Cambro-Ordovician Ollo de Sapo magmatism in the Iberian Massif and its Variscan evolution: A review. *Earth-Science Reviews, 176,* 345–372.

Geological Map of Switzerland, 1:500000. (2008). Federal Office of Topography swisstopo. Retrieved April 5, 2020, from http://www.map.geo.admin.ch.

Giobbi Mancini, E., Boriani, A., & Villa, I. M. (2003). Pre-Alpine ophiolites in the basement of Southern Alps: the presence of a bimodal association (LAG-Leptyno-Amphibolitic group) in the Serie dei Laghi (N-Italy, Ticino-CH). *Rendiconti lincei, Scienze fisiche e naturali, 14*(s9), 79–99.

Gnägi, C., & Labhart, T.P. (2015). *Geologie der Schweiz.* 9. Auflage, Ott Verlag.

Goodge, J. W. (2007). Metamorphism in the Ross orogen and its bearing on Gondwana margin tectonics. *Geological Society of America Special Paper, 419,* 185–203.

Graeter, P. (1951). Geologie und Petrographie des Malcantone (südliches Tessin). *Schweizerische Mineralogische und Petrographische Mitteilungen, 31,* 361–482.

Handy, M. R., Franz, L., Heller, F., Janott, B., & Zurbriggen, R. (1999). Multistage accretion and exhumation of the continental crust (Ivrea crustal section, Italy and Switzerland). *Tectonophysics, 18,* 1154–1177.

Harris, N.B.W., Pearce, J.A., & Tindle, A.G. (1986). Geochemical characteristics of collision-zone magmatism. In M.P. Coward, & A,C, Ries (Eds.), *Collision Tectonics* (Vol. 19, pp. 67–81). Geological Society Special Publication, London.

Hauser, A., & Zurbriggen, R. (1994). Geology of the crystalline basement of the Hadbin area (Salalah area, Dhofar, Sultanate of Oman). *Schweizerische Mineralogische und Petrographische Mitteilungen, 74,* 213–226.

Heim, A. (1921). *Geologie der Schweiz. Band II: Die Schweizer Alpen. Erste Hälfte* (pp. 0–476). Leipzig.

Heim, A. (1922). *Geologie der Schweiz. Band II: Die Schweizer Alpen. Zweite Hälfte* (pp. 477–1018). Leipzig.

Heinisch, H. (1981). Zum ordovizischen „Porphyroid"-Vulkanismus der Ost- und Südalpen, Stratigraphie, Petrographie. *Geochemie. Jahrbuch der Geologischen Bundesanstalt., 124*(1), 1–109.

Hoinkes, G., & Thöni, M. (1993). Evolution of the Ötztal-Stubai, Scarl-Campo and Ulten basement units. In J. F. Von Raumer & F. Neubauer (Eds.), *Pre-mesozoic geology in the Alps* (pp. 485–494). Heidelberg: Springer.

Hu, P. Y., Zhai, Q. G., Jahn, B. M., Wang, J., Li, C., Lee, H. Y., et al. (2015). Early Ordovician granites from the South Qiangtang terrane, northern Tibet: Implications for the early Paleozoic tectonic evolution along the Gondwanan proto-Tethyan margin. *Lithos, 220–223,* 318–338.

Irving, T. N., & Baragar, W. A. R. (1971). A guide to the chemical classification of the common volcanic rocks. *Canadian Journal of Earth Sciences, 8,* 523–548.

Koralay, O. E., Candan, O., Chen, F., Akal, C., Oberhänsli, R., Satır, M., et al. (2012). Pan-African magmatism in the Menderes Massif: geochronological data from leucocratic tourmaline orthogneisses in western Turkey. *International Journal of Earth Sciences (Geologische Rundschau), 101,* 2055–2081.

Kröner, A., & Stern, R.J. (2004). *Pan-African Orogeny.* Encyclopedia of Geology (Vol. 1). Amsterdam: Elsevier.

Labhart, T.P. (1977). *Aarmassiv und Gotthardmassiv. Geologisch-tektonische Übersicht. 1:200'000.* Sammlung geologischer Führer, Band 63.

Laumonier, M., Scaillet, B., Pichavant, M., Champallier, R., Andujar, J., & Arbaret, L. (2014). On the conditions of magma mixing and its bearing on andesite production in the crust. *Nature Communications, 5,* 5607. https://doi.org/10.1038/ncomms6607.

Le Maitre, R. W. (1976). The chemical variability of some common igneous rocks. *Journal of Petrology, 17,* 589–637.

Li, L., Lin, S., Xing, G., Jiang, Y., & He, J. (2017). First direct evidence of Pan-African Orogeny associated with Gondwana Assembly in the Cathaysia Block of Southern China. *Scientific Reports, 7,* 794. https://doi.org/10.1038/s41598-017-00950-x.

Lin, Y.-L., Yeh, M.-W., Lee, T.-Y., Chung, S.-L., Iizuka, Y., & Charusiri, P. (2013). First evidence of the Cambrian basement in Upper Peninsula of Thailand and its implication for crustal and tectonic evolution of the Sibumasu terrane. *Gondwana Research, 24,* 1031–1037.

Linnemann, U. (2007). Ediacaran rocks from the Cadomian basement of the Saxo-Thuringian Zone (NE Bohemian Massif, Germany): age constraints, geotectonic setting and basin development. *Geological Society, London, Special Publications, 286,* 35–51. https://doi.org/10.1144/SP286.4.

Linnemann, U., Gerdes, A., Hofmann, M., & Marko, L. (2014). Neoproterozoic to early Cambrian crustal growth and orogenic zoning along the periphery of the West African Craton-Constraints from U-Pb zircon ages and Hf isotopes (Schwarzburg Antiform, Germany). *Precambrian Research, 244,* 236–278.

Maniar, P. D., & Piccoli, P. M. (1989). Tectonic discrimination of granitoids. *Bulletin of the Geological Society of America, 101,* 635–643.

Mercolli, I., Biino, G. G., & Abrecht, J. (1994). The lithostratigraphy of the pre-Mesozoic basement of the Gotthard massif: A review. *Schweizerische Mineralogische und Petrographische Mitteilungen, 74,* 29–40.

Mercolli, I., Briner, A. P., Frei, R., Schönberg, R., Nägler, T. F., Kramers, J., et al. (2006). Lithostratigraphy and geochronology of the Neoproterozoic crystalline basement of Salalah, Dhofar, Sultanate of Oman. *Precambrian Research, 145,* 182–206.

Oberli, F., Meier, M., & Biino, G. (1994). Time constraints on the pre-Variscan magmatic/metamorphic evolution of the Gotthard and Tavetsch units derived from single-zircon U-Pb results. *Schweizerische Mineralogische und Petrographische Mitteilungen, 74,* 483–488.

Österle, J. E., Klötzli, U., Stockli, D. F., Palzer-Khomenko, M., & Kanjanapayont, P. (2019). New age constraints on the Lan Sang gneiss complex, Thailand, and the timing of activity of the Mae Ping shear zone from in situ and

depth-profile zircon and monazite U-Th-Pb geochronology. *Journal of Asian Earth Sciences, 181,* 103886.

Pearce, J. A., Harris, N. B. W., & Tindle, A. G. (1984). Trace element discrimination for the tectonic interpretation of granitic rocks. *Journal of Petrology, 25*(4), 956–983.

Pettijohn, F.J. (1963). Chemical composition of sandstones—excluding carbonate and volcanic sands. *U. S. Geological Survey, Professional Paper, 440-S.*

Pinarelli, L., Bergomi, M. A., Boriani, A., & Giobbi, E. (2008). Pre-metamorphic melt infiltration in metasediments: geochemical, isotopic (Sr, Nd, and Pb), and field evidence from Serie dei Laghi (Southern Alps, Italy). *Mineralogy and Petrology, 93,* 213–242. https://doi.org/10.1007/s00710-007-0222-4.

Pouclet, A., Álvaro, J. J., Bardintzeff, J.-M., Gil Imaz, A., Monceret, E., & Vizcaïno, D. (2016). Cambrian-early Ordovician volcanism across the South Armorican and Occitan domains of the Variscan Belt in France: Continental breakup and rifting of the northern Gondwana margin. *Geoscience Frontiers, 8*(1), 25–64. https://doi.org/10.1016/j.gsf.2016.03.002.

Rino, S., Kon, Y., Sato, W., Maruyama, S., Santosh, M., & Zhao, D. (2008). The Grenvillian and Pan-African orogens: world's largest orogenies through geologic time, and their implications on the origin of superplume. *Gondwana Research, 14,* 51–72.

Rossetti, F., Nozaem, R., Lucci, F., Vignaroli, G., Gerdes, A., Nasrabadi, M., et al. (2015). Tectonic setting and geochronology of the Cadomian (Ediacaran-Cambrian) magmatism in Central Iran, Kuh-e-Sarhangi region (NW Lut Block). *Journal of Asian Earth Sciences, 102,* 24–44.

Rossi, J. N., Toselli, A. J., Saavedra, J., Sial, A. N., Pellitero, E., & Ferreira, V. P. (2002). Common crustal source for contrasting peraluminous facies in the early Paleozoic Capillitas batholith, NW Argentina. *Gondwana Research, 5*(2), 325–337.

Santosh, M., Maruyama, S., Sawaki, Y., & Meert, J. G. (2014). The Cambrian Explosion: Plume-driven birth of the second ecosystem on Earth. *Gondwana Research, 25,* 945–965.

Schaltegger, U., Abrecht, J., & Corfu, F. (2003). The Ordovician orogeny in the Alpine basement: constraints from geochronology and geochemistry in the Aar Massif (Central Alps). *Schweizerische Mineralogische und Petrographische Mitteilungen, 83,* 183–195.

Schmitt, R. S., Trouw, R. A. J., Van Schmus, W. R., & Pimentel, M. M. (2004). Late amalgamation in the central part of West Gondwana: new geochronological data and the characterization of a Cambrian collisional orogeny in the Ribeira Belt (SE Brazil). *Precambrian Research, 133,* 29–61.

Schwartz, J. J., Gromet, L. P., & Miro, R. (2008). Timing and Duration of the Calc-Alkaline Arc of the Pampean Orogeny: Implications for the Late Neoproterozoic to Cambrian Evolution of Western Gondwana. *The Journal of Geology, 116,* 39–61. https://doi.org/10.1086/524122.

Schwindinger, M., & Weinberg, R. F. (2017). A felsic MASH zone of crustal magmas—Feedback between granite magma intrusion and in situ crustal anatexis. *Lithos, 284–285,* 109–121.

Shafaii Moghadam, H., Khademi, M., Hu, Z., Stern, R. J., Santos, J. F., & Wu, Y. (2015). Cadomian (Ediacaran–Cambrian) arc magmatism in the Chah-Jam–Biarjmand metamorphic complex (Iran): Magmatism along the northern active margin of Gondwana. *Gondwana Research, 27,* 439–452.

Siebel, W., Raschka, H., Irber, W., Kreuzer, H., Lenz, K. L., Höhndorf, A., et al. (1997). Early Paleozoic acid magmatism in the Saxothuringian belt: new insights from a geochemical and isotopic study of orthogneisses and metavolcanics rocks from the Fichtelgebirge, SE Germany. *Journal of Petrology, 38,* 203–230.

Siegesmund, S., Oriolo, S., Heinrichs, T., Basei, M. A. S., Nolte, N., Hüttenrauch, F., et al. (2018). Provenance of Austroalpine basement metasediments: tightening up Early Palaeozoic connections between peri-Gondwanan domains of central Europe and Northern Africa. *International Journal of Earth Sciences, 107*(6), 2293–2315.

Spicher, A. (1940). Geologie und Petrographie des oberen Val d'Isone (südliches Tessin). *Schweizerische Mineralogische und Petrographische Mitteilungen, 20,* 17–100.

Squire, R. J., Campbell, I. H., Allen, C. M., & Wilson, C. J. L. (2006). Did the Transgondwanan Supermountain trigger the explosive radiation of animals on Earth? *Earth and Planetary Science Letters, 250,* 116–133.

Stephan, T., Kroner, U., Romer, R. L., & Rösel, D. (2019). From a bipartite Gondwanan shelf to an arcuate Variscan belt: The early Paleozoic evolution of northern Peri-Gondwana. *Earth-Science Reviews, 192,* 491–512.

Thöny, W. F., Tropper, P., Schennach, F., Krenn, E., Finger, F., Kaindl, R., et al. (2008). The metamorphic evolution of migmatites from the Ötztal complex (Tyrol, Austria) and constraints on the timing of the pre-Variscan high-T event in the Eastern Alps. *Swiss Journal of Geosciences, 101*(1), 111–126.

Timm, C., Davy, B., Haase, K., Hoernle, K. A., Graham, I. J., de Ronde, C. E. J., et al. (2014). Subduction of the oceanic Hikurangi Plateau and its impact on the Kermadec arc. *Nature Communications, 5,* 4923. https://doi.org/10.1038/ncomms5923.

Torsvik, T.H., & Cocks, L.R.M. (2011). The Paleozoic paleogeography of central Gondwana. In D.J.J. Van Hinsbergen, S.J.H. Buiter, T.H. Torsvik, C. Gaina, & S.J. Webb (Eds.), *The formation and evolution of Africa: a synopsis of 3.8 Ga of earth history* (Vol. 357, pp. 137–166). London: Geological Society, Special Publications.

Ustaömer, P. A., Ustaömer, T., Collins, A. S., & Robertson, A. H. F. (2009). Cadomian (Ediacaran–Cambrian) arc magmatism in the Bitlis Massif, SE Turkey: Magmatism along the developing northern margin of Gondwana. *Tectonophysics, 473,* 99–112.

Vielzeuf, D., & Holloway, J. R. (1988). Experimental determination of the fluid-absent melting relations in the pelitic system. Consequences for crustal differentiation. *Contributions to Mineralogy and Petrology, 98,* 257–276.

Villaros, A., Laurent, O., Couzinié, S., Moyen, J.-F., & Mintrone, M. (2018). Plutons and domes: the consequences of anatectic magma extraction—example from the southeastern French Massif Central. *International Journal of Earth Sciences, 107,* 2819–2842.

Villaseca, C., Barbero, L., & Herreros, V. (1998). A re-examination of the typology of peraluminous granite types in intracontinental orogenic belts. *Transactions of the Royal Society of Edinburgh: Earth Sciences, 89,* 113–119.

Villaseca, C., Merino Martínez, E., Orejana, D., Andersenc, T., & Belousova, E. (2016). Zircon Hf signatures from granitic orthogneisses of the Spanish Central System: significance and sources of the Cambro-Ordovician magmatism in the Iberian Variscan Belt. *Gondwana Research, 34,* 60–83.

Von Raumer, J. F., Bussy, F., Schaltegger, U., Schulz, B., & Stampfli, G. M. (2013). Pre-Mesozoic Alpine basements: their place in the European Paleozoic framework. *Bulletin of the Geological Society of America, 125*(1–2), 89–108.

Von Raumer, J. F., Stampfli, G. M., Arenas, R., & Sanchez Martinez, S. (2015). Ediacaran to Cambrian oceanic rocks of the Gondwana margin and their tectonic interpretation. *International Journal of Earth Sciences, 104,* 1107–1121.

Von Raumer, J. F., Stampfli, G. M., & Bussy, F. (2003). Gondwana-derived microcontinents—the constituents of the Variscan and Alpine collisional orogens. *Tectonophysics, 365,* 7–22.

White, A. J. R., & Chappell, B. W. (1990). Per migma ad magma downunder. *Geological Journal, 25,* 221–225.

Winter, J. D. (2010). *An introduction to igneous and metamorphic petrology* (2nd ed.). New York: Prentice Hall.

Zurbriggen, R. (1996). Crustal genesis and uplift history of the Strona-Ceneri zone (Southern Alps). *Unpublished PhD thesis, University of Bern, Switzerland.*

Zurbriggen, R. (2015). Ordovician orogeny in the Alps: a reappraisal. *International Journal of Earth Sciences (Geologische Rundschau), 104,* 335–350. https://doi.org/10.1007/s00531-014-1090-x.

Zurbriggen, R. (2017). The Cenerian orogeny (early Paleozoic) from the perspective of the Alpine region. *International Journal of Earth Sciences (Geologische Rundschau), 106,* 517–529. https://doi.org/10.1007/s00531-016-1438-5.

Zurbriggen, R., Franz, L., & Handy, M. R. (1997). Pre-Variscan deformation, metamorphism and magmatism in the Strona-Ceneri Zone (southern Alps of northern Italy and southern Switzerland). *Schweizerische Mineralogische und Petrographische Mitteilungen, 77,* 361–380.

Zurbriggen, R., Kamber, B. S., Handy, M. R., & Nägler, T. F. (1998). Dating synmagmatic folds: a case study of Schlingen structures in the Strona-Ceneri Zone (Southern Alps, northern Italy). *Journal of Metamorphic Geology, 16,* 403–414.

Publisher's Note